RedFame

Applied Economics and Finance
Vol. 7, No. 6; November 2020
ISSN 2332-7294 E-ISSN 2332-7308
Published by Redfame Publishing
URL: http://aef.redfame.com

Distributionally Robust XVA via Wasserstein Distance: Wrong Way Counterparty Credit and Funding Risk

Derek Singh[1] & Shuzhong Zhang[1]

[1] Department of Industrial and Systems Engineering, University of Minnesota, United States

Correspondence: Derek Singh, Department of Industrial and Systems Engineering, University of Minnesota, United States.

Received: September 22, 2020 Accepted: October 14, 2020 Available online: October 27, 2020

doi:10.11114/aef.v7i6.5060 URL: https://doi.org/10.11114/aef.v7i6.5060

Abstract

This paper investigates calculations of robust X-Value adjustment (XVA), in particular, credit valuation adjustment (CVA) and funding valuation adjustment (FVA), for over-the-counter derivatives under distributional ambiguity using Wasserstein distance as the ambiguity measure. Wrong way counterparty credit risk and funding risk can be characterized (and indeed quantified) via the robust XVA formulations. The simpler dual formulations are derived using recent Lagrangian duality results. Next, some computational experiments are conducted to measure the additional XVA charges due to distributional ambiguity under a variety of portfolio and market configurations. Finally some suggestions for further work are discussed.

Keywords: OTC, CCR, CVA, FVA, derivatives, distributionally robust optimization, Wasserstein distance, duality

1. Introduction and Overview

1.1 Financial Markets Context and Background

An X-Value adjustment (XVA) is a generic term used to refer to various valuation adjustments, typically applied to over-the-counter (OTC) derivatives held by financial institutions. The first of the XVAs, and still one of the most significant, in terms of market exposure, is credit valuation adjustment (CVA). One of the more recent, and perhaps equally significant, exposures is funding valuation adjustment (FVA). Both of these XVAs have similar structure (unilateral, bilateral) and mathematical form for computation. Other XVAs include capital valuation adjustment (KVA) and margin valuation adjustment (MVA). Wrong way risk refers to adversely correlated moves in the market exposures and the counterparty spreads (e.g. credit, funding). It can materially affect the magnitude of the XVA adjustment.

CVA represents the impact on portfolio market value due to counterparty default. Unilateral CVA can be represented mathematically as an integral of discounted expected positive exposure times (incremental) counterparty default probability. The market valuation adjustment is a function of counterparty credit risk, the underlying (market) risk factors that drive the portfolio valuation (and hence positive exposure), as well as the correlations between these market risk factors and the counterparty credit risk curves for a given portfolio. CVA is typically measured and reported at the counterparty level.

The “other side” of unilateral CVA is unilateral debit valuation adjustment (DVA). This is the benefit to the firm of its reduced liability due to its own default. As above, the market valuation adjustment is a function of firm credit risk, underlying market risk factors that drive portfolio valuation, and the correlations. Unilateral DVA can be represented mathematically as an integral of discounted negative exposure times (incremental) firm default probability. DVA is typically measured at the firm level.

Bilateral CVA represents the dual impact on portfolio market value due to counterparty default and firm default. Bilateral CVA can be represented mathematically as the difference between two integrals: (i) discounted expected positive exposure times (incremental) counterparty default probability prior to firm default, (ii) discounted expected negative exposure times (incremental) firm default probability prior to counterparty default. Bilateral CVA is typically measured and reported at the counterparty level, for a given firm.

FVA represents the impact on portfolio market value due to funding exposures for the hedge on uncollateralized derivatives. It represents the market valuation adjustment due to funding exposure risk. Funding cost adjustment (FCA)

can be represented mathematically as an integral of discounted expected positive exposure times funding cost (incremental) conditional on joint counterparty and firm survival. FCA arises for a positive portfolio exposure since this implies a negative hedge exposure which leads to a funding cost for collateral posted. The market valuation adjustment is a function of joint counterparty and firm credit risk, the underlying (market) risk factors that drive the portfolio valuation (and hence positive exposure) as well as funding cost, as well as the correlations between these market risk factors and the credit risk curves for a given portfolio. FCA is typically measured and reported at the funding netting set level.

The "other side" of FCA is funding benefit adjustment (FBA). This represents the funding benefit to the firm, for interest income proceeds on received collateral posted against counterparty exposure on the hedge, as measured by discounted expected negative exposure times funding benefit conditional on joint counterparty and firm survival. As above, the market valuation adjustment is a function of counterparty and firm credit risk, underlying market risk factors that drive portfolio valuation and funding benefit, and the correlations. FBA can be represented mathematically as an integral of discounted negative exposure times funding benefit conditional on joint counterparty and firm survival. FBA is typically measured at the funding netting set level.

(Bilateral) FVA represents the dual impact on portfolio market value due to both funding cost and funding benefit exhibited over the portfolio lifetime. FVA can be represented mathematically as the difference (or sum) of two integrals: (i) discounted expected positive exposure times funding cost conditional on joint counterparty and firm survival (ii) discounted expected negative exposure times funding benefit conditional on joint counterparty and firm survival. FVA is typically measured and reported at the netting set level for a given firm.

U.S. regulatory authorities, the Federal Reserve and Office of the Comptroller of the Currency (OCC), periodically assess national banks' compliance with Market Risk Capital Rule (MRR). Counterparty credit risk (CCR) and funding risk (FR) metrics are key metrics used to evaluate bank risk profiles and balance sheet exposures due to over the counter (OTC) derivatives, securities financing transactions, and other transactions and exposures (Office of the Comptroller of the Currency, 2011). Basel Committee on Banking Supervision has issued supervisory guidance, in the form of its Basel III framework (and supplemental guidance), to quantify capital charges due to CCR. A new element in Basel III was a capital charge due to degradation in CCR for a given portfolio or book of business (Basel Committee on Banking Supervision, 2015). Potential revisions to the Basel framework may include elements to quantify CCR capital charges due to deterioration in market risk exposure.

The Dodd-Frank Wall Street Reform and Consumer Protection Act (July 2010) enacted regulations for the swaps market and authorized creation of centralized exchanges for swaps (and other) derivatives trading. Derivatives that trade on an exchange reference the exchange as the transaction counterparty. Since exchanges clear multiple (typically offsetting) transactions and hedge their risk through other third parties, exchange traded derivatives have minimal CCR risk profile. However, OTC derivatives typically have banks or other financial institutions as counterparties which do have material credit risk profiles. According to International Swap Dealers Association (ISDA) the OTC derivatives notional outstanding was 544 trillion at year end 2018. Interest rate derivatives notional outstanding was 437 trillion at year end 2018. Recent (04/20/20) Bloomberg CDX investment grade and high yield credit spreads are 93 and 643 basis points respectively. Consequently the CCR and FR exposures (due to uncollateralized or partially collateralized hedges) inherent in the OTC derivatives market represent significant market risk exposures. This motivates the concepts of worst case CVA , FVA, and wrong way risk (WWR) and the impact of ambiguity in probability distribution on these exposures and risk metrics. It is these considerations that motivate this line of research (Ramzi Ben-Abdallah and Marzouk, 2019), (El Hajjaji and Subbotin, 2015).

Distributional ambiguity is characterized via the Wasserstein metric for a couple of reasons. The Wasserstein metric is a (reasonably) well understood metric and a natural, intuitive way to compare two probability distributions using ideas of transport cost. It is also a flexible approach that encompasses parametric and non-parametric distributions of either discrete or continuous form. For example, one can explore distributions that alter the shape of the marginals as well as the correlation structure. Furthermore, recent duality results and structural results on the worst case distributions can help us to better understand and/or quantify the market model transitions as well as measure (in a relative sense) the degree of wrong way risk inherent to a given market model.

An outline of this paper is as follows. We begin with an overview of CVA, FVA, and WWR as well as a literature review. Next, the main theoretical results of the paper are developed. Following that, there is a computational study of wrong way risk for a representative set of derivative portfolios and market environments. In the last part, we discuss conclusions and suggestions for further research. All detailed proofs of propositions, corollaries, and theorems are deferred to the Appendix.

1.2 Literature Review

The authors are not aware of any substantial research that has been done on the topic of worst case FVA. The discussion below pertains to literature regarding worst case CVA. In the past few years some research has been done to investigate and quantify the effect of distributional ambiguity on CVA. Brigo et al. (2013) explicitly incorporate correlation into the stochastic processes driving the market risk and credit default factors. They quantify the effect of dependency structure (and hence wrong way risk) on CVA for a variety of asset classes: interest rate swaps, interest rate swaptions, commodities, equities, and foreign exchange products. Glasserman and Yang (2015) bound the effect of wrong way risk on CVA. Their approach considers a discrete setting for portfolio exposures and counterparty default times and formulates worst case CVA as the solution to a worst case linear program subject to certain constraints (such as fixed marginals for portfolio exposures and default times), where the dependency structure across the risk factors is allowed to vary. As this approach leads to large values for worst case CVA, they introduce a penalty term to modulate or temper the degree of wrong way risk and run some sensitivity analysis to study the effect of the penalty term. Kullback-Leibler (KL) divergence is used to measure the distance between the reference (empirical) and the perturbed distribution. They remark that determining a suitable value for the penalty term would be a topic for further research.

Memartoluie, in his PhD thesis, uses an ordered scenario copula methodology to quantify worst case CVA (Memartoluie, 2017). A particular method of scenario ordering correlates portfolio exposures to company default times (firm, counterparty, or both) and the resulting dependency structure introduces wrong way risk. He chooses to order exposure scenarios by increasing time averaged total exposure and then simulates company default times conditional on the exposure path using pre-specified correlation between the market risk factor(s) and credit risk factor(s). For worst case correlations set to one, he finds results for worst case CVA that are comparable to the method of Glasserman and Yang. In a recent paper, Ben-Abdallah et al. perform a computational study on the effect of wrong way risk on CVA for a portfolio of interest rate swaps, caps, and floors (Ramzi Ben-Abdallah and Marzouk, 2019). They find that the dependency structure between interest rates and default intensity produces material wrong way risk whereas the dependency structure between interest rate volatility and default intensity does not.

Recent results in Lagrangian duality were independently developed by Blanchet and Murthy (2019) and Gao and Kleywegt (2016). These results hold under mild assumptions such as upper semicontinuity in the objective function and lower semicontinuity in the distance function. Blanchet et al. (2016a) applied this duality theory to study a number of classical regression problems in machine learning under distributional ambiguity. In that context, the authors find that distributional ambiguity can be viewed as adding a regularization term to the objective function, analogous to a penalized regression setting. Similarly, Gao et al. (2017) apply the Lagrangian duality theory to problems in statistical learning.

The main innovation in our work is to apply these recent results in Lagrangian duality to worst case CVA and FVA using Wasserstein distance as the ambiguity measure. Furthermore, analytical expressions are derived for the solutions to the inner and outer convex optimization problems that comprise worst case CVA and FVA via the Wasserstein approach. A computational study shows the material impact of distributional ambiguity on worst case CVA and FVA, illustrates the risk profiles, and computes the worst case distributions.

1.3 Preliminary Material

1.3.1 Restatement of Lagrangian Duality Result

As in our earlier work this year, (Singh and Zhang, 2020) a key step in the approach is to use recent Lagrangian duality results to formulate the equivalent dual problems. The dual problems are much more tractable than the primal problems since they only involve the reference probability measure as opposed to a Wasserstein ball of probability measures (of some finite radius). For real valued upper semicontinuous objective function $f \in L^1$ and non-negative lower semicontinuous cost function c such that $\{(u,v) : c(u,v) < \infty\}$ is Borel measurable and non-empty, it holds that (Blanchet et al., 2016b)

$$\sup_{Q \in \mathscr{U}_\delta(Q_N)} \mathbb{E}^Q[f(X)] = \inf_{\lambda \geq 0} [\lambda \delta + \frac{1}{N} \sum_{i=1}^{n} \Psi_\lambda(x_i)] \tag{1}$$

where

$$\Psi_\lambda(x_i) := \sup_{u \in dom(f)} [f(u) - \lambda c(u, x_i)]. \tag{2}$$

Further details, including proofs and concrete examples, can be found in the papers by Blanchet and Murthy (2019), Gao and Kleywegt (2016), and Esfahani and Kuhn (2018). These authors independently derived these results around the same time although Blanchet and Murthy (2019) did so in a more general setting.

1.3.2 Characterization of Worst Case Distributions Simply put, the set of worst case distributions (when non-empty) can

be defined as $WC(f,\delta) := \{Q^* : \mathbb{E}^{Q^*}[f(X)] = \sup_{Q\in\mathscr{U}_\delta(Q_N)} \mathbb{E}^{Q}[f(X)]\}$. Another recent set of results from the literature describes the structure of the worst case distribution(s) when they exist (Blanchet and Murthy, 2019), (Gao and Kleywegt, 2016), (Esfahani and Kuhn, 2018). The boundedness conditions for existence are tied to the growth rate $\kappa := \limsup_{d(X,X_0)\to\infty} \frac{f(X)-f(X_0)}{d(X,X_0)}$ for fixed X_0 and the value of the dual minimizer λ^*. For empirical reference distributions, supported on N points, such that $WC(f,\delta)$ is non-empty, there exists *a* worst case distribution that is *another* empirical distribution supported on at most $N+1$ points. This worst case distribution can be constructed via a greedy approach. For up to N points, they can be identified as solving $x_i^* \in_{\tilde{x}\in dom(f)} [\lambda^* c(\tilde{x},x_i) - f(\tilde{x})]$. At most one point has its probability mass split into two pieces (according to budget constraint δ) that solve $x_{i_0}^*, x_{i_0}^{**} \in_{\tilde{x}\in dom(f)} [\lambda^* c(\tilde{x},x_{i_0}) - f(\tilde{x})]$. Details can be found in Gao and Kleywegt (2016).

1.3.3 Bilateral CVA Notation and core definitions for bilateral CVA problem setup incorporate those for unilateral CVA and DVA. Bilateral CVA measures expected portfolio loss (or benefit) due to counterparty and/or firm default. Let $V^+(\tau_C)$ denote the discounted positive portfolio exposure at time τ_C and let $R_C \in [0,1)$ denote the recovery rate the firm receives upon counterparty default. Let $V^-(\tau_F)$ denote the discounted negative portfolio exposure at time τ and let $R_F \in [0,1)$ denote the recovery rate the counterparty receives upon firm default. The problem setup here assumes a fixed set of observation dates, $0 = t_0 < t_1 < \cdots < t_n = T$. Let X^+ denote the vector of recovery adjusted discounted positive exposures and Y_C denote the vector of counterparty default indicators. Let (x_i^+, y_i^c) denote realizations of (X^+, Y_C) along sample paths for $i = \{1,2,\ldots,N\}$. Let X^- denote the vector of recovery adjusted discounted firm negative exposures and Y_F denote the vector of firm default indicators. Let (x_i^-, y_i^f) denote realizations of (X^-, Y_F) along sample paths for $i = \{1,2,\ldots,N\}$.

Due to the linkage, one can write $X = X^+ + X^-$ and decompose sample realizations of X accordingly. Therefore, let (x_i, y_i^c, y_i^f) denote realizations of (X, Y_C, Y_F) along sample paths for $i = \{1,2,\ldots,N\}$. The relation $x_i = x_i^+ + x_i^-$ can be used to decompose x_i into its positive and negative exposures respectively.

The bilateral CVA associated with discounted positive exposure $V^+(\tau_C)$, counterparty default indicator $\mathbb{1}_{\{\tau_C\le T\}\cap\{\tau_C<\tau_F\}}$, discounted negative exposure $V^-(\tau_F)$, firm default indicator $\mathbb{1}_{\{\tau_F\le T\}\cap\{\tau_F<\tau_C\}}$, is

$$CVA^{\mathrm{B}} = \mathbb{E}[(1-R_C)V^+(\tau_C)\mathbb{1}_{\{\tau_C\le T\}\cap\{\tau_C<\tau_F\}}] + \mathbb{E}[(1-R_F)V^-(\tau_F)\mathbb{1}_{\{\tau_F\le T\}\cap\{\tau_F<\tau_C\}}]. \tag{3}$$

Equivalently, one can write

$$CVA^{\mathrm{B}} = (1-R_C)\int_0^T \mathbb{E}[V^+(t)|\tau_C = t, \tau_F > t]d\Pi_C'(t) + (1-R_F)\int_0^T \mathbb{E}[V^-(t)|\tau_F = t, \tau_C > t]d\Pi_F'(t), \tag{4}$$

where the joint counterparty and firm default time distributions are given by $\Pi_C'(t) = P(\tau_C \le t, \tau_F > \tau_C)$ and $\Pi_F'(t) = P(\tau_F \le t, \tau_C > \tau_F)$ (Green, 2015), (Lichters et al., 2015), (Memartoluie, 2017). The pair of vectors $(X^+, Y_C) \in (\mathbb{R}_+^n \times B_n^1)$ is

$$X^+ = ((1-R_C)V^+(t_1),\ldots,(1-R_C)V^+(t_n)) \quad and \quad Y_C = (\mathbb{1}_{\{\tau_C=t_1\}\cap\{\tau_F>\tau_C\}},\ldots,\mathbb{1}_{\{\tau_C=t_n\}\cap\{\tau_F>\tau_C\}}), \tag{5}$$

and the pair of vectors $(X^-, Y_F) \in (\mathbb{R}_-^n \times B_n^1)$ is

$$X^- = ((1-R_F)V^-(t_1),\ldots,(1-R_F)V^-(t_n)) \quad and \quad Y_F = (\mathbb{1}_{\{\tau_F=t_1\}\cap\{\tau_C>\tau_F\}},\ldots,\mathbb{1}_{\{\tau_F=t_n\}\cap\{\tau_C>\tau_F\}}). \tag{6}$$

Here B_n^1 denotes the set of default time vectors: binary vectors of ones and zeros with n components, and at most one non-zero element. Note that counterparty or firm default occurs on at most one observation date within the fixed set of dates in the problem setup. The empirical measure Φ_N, in terms of Dirac measure $\delta_{(x_i,y_i^c,y_i^f)}$, is

$$\Phi_N := \frac{1}{N}\sum_{i=1}^N \delta_{(x_i,y_i^c,y_i^f)}. \tag{7}$$

Under the empirical measure, Φ_N, bilateral CVA is a sum of expectations of inner products

$$CVA^{\mathrm{B}} = \mathbb{E}^{\Phi_N}[\langle X^+, Y_C\rangle] + \mathbb{E}^{\Phi_N}[\langle X^-, Y_F\rangle]. \tag{8}$$

In the context of this work, the ambiguity set for probability measures is

$$\mathscr{U}_{\delta_3}(\Phi_N) = \{P : D_c(\Phi, \Phi_N) \le \delta_3\} \tag{9}$$

where D_c is the optimal transport cost or Wasserstein discrepancy for cost function c (Blanchet et al., 2018). For conve-

nience the definition for D_c is given as

$$D_c(\Phi,\Phi') = \inf\{\mathbb{E}^{\pi}[c(\xi_A,\xi_B)] : \pi \in \mathscr{P}(\mathbb{R}^d \times \mathbb{R}^d), \xi_A \sim \Phi, \xi_B \sim \Phi'\} \tag{10}$$

where π belongs to the set of joint distributions with marginals Φ and Φ'. Here ξ_A denotes $(X_A, Y_A^C, Y_A^F) \in (\mathbb{R}^n \times B_n^1 \times B_n^1)$ and ξ_B denotes $(X_B, Y_B^C, Y_B^F) \in (\mathbb{R}^n \times B_n^1 \times B_n^1)$ respectively. The analysis in this work uses the cost function c_{S_3} where

$$c_{S_3}((u,v_1,v_2),(x,y_1,y_2)) = S_3\langle v_1 - y_1, v_1 - y_1\rangle + S_3\langle v_2 - y_2, v_2 - y_2\rangle + \langle u - x, u - x\rangle. \tag{11}$$

The scale factor $S_3 > 0$ is used to compensate for different domains: $(u,v_1,v_2) \in (\mathbb{R}^n \times B_n^1 \times B_n^1), (x,y_1,y_2) \in (\mathbb{R}^n \times B_n^1 \times B_n^1)$.

1.3.4 Unilateral CVA, DVA

Bilateral CVA can be reduced to express unilateral CVA as

$$CVA^{\mathrm{U}} = \mathbb{E}[(1-R_C)V^+(\tau_C)\mathbb{1}_{\{\tau_C \le T\}}] = (1-R_C)\int_0^T \mathbb{E}[V^+(t)|\tau_C = t]d\Pi_C(t), \tag{12}$$

where the counterparty default time distribution is given by $\Pi_C(t) = P(\tau_C \le t)$. Note the assumption here is that $\tau_C < \tau_F$. Similarly, it can be reduced to express unilateral DVA (note the minus sign), assuming $\tau_F < \tau_C$, as

$$DVA^{\mathrm{U}} = -\mathbb{E}[(1-R_F)V^-(\tau_F)\mathbb{1}_{\{\tau_F \le T\}}] = -(1-R_F)\int_0^T \mathbb{E}[V^-(t)|\tau_F = t]d\Pi_F(t), \tag{13}$$

where firm default time distribution is given by $\Pi_F(t) = P(\tau_F \le t)$ (Green, 2015), (Lichters et al., 2015), (Memartoluie, 2017).

1.3.5 FVA

Notation and core definitions for (bilateral) FVA problem setup incorporate those for FCA and FBA. FVA measures expected funding costs and benefits over portfolio lifetime. Let $V^+(t)$ denote the positive portfolio exposure at time t. Let $V^-(t)$ denote the negative portfolio exposure at time t. The problem setup here assumes a fixed set of observation dates, $0 = t_0 < t_1 < \cdots < t_n = T$. Let X^+ denote the vector of discounted positive exposures and Y_C denote the vector of counterparty survival indicators. Let X^- denote the vector of discounted negative exposures and Y_F denote the vector of firm survival indicators. Further, let Y_{CF} denote the Hadamard product $Y_C \odot Y_F$ which represents the vector of joint survival indicators. To incorporate funding, let Z^+ denote the vector of funding costs incurred on exposures X^+. And similarly for Z^- with respect to exposures X^-. Due to the linkage between Z^+ and Z^-, one can write $Z = Z^+ + Z^-$ and decompose sample realizations of Z into Z^+ and Z^- accordingly. Therefore, let (z_i, y_i^{cf}) denote realizations of (Z, Y_{CF}) along sample paths for $i = \{1,2,\ldots,N\}$. The relation $z_i = z_i^+ + z_i^-$ can be used to decompose z_i into its positive and negative exposures respectively.

The FVA associated with funding costs $Z(t)$, joint survival indicator $\mathbb{1}_{\{\tau_C > t\}\cap\{\tau_F > t\}}$ is (Lichters et al., 2015), (Green, 2015)

$$FVA = FCA + FBA = \int_0^T \mathbb{E}[Z^+(t)\mathbb{1}_{\{\tau_C>t\}\cap\{\tau_F>t\}}]dt + \int_0^T \mathbb{E}[Z^-(t)\mathbb{1}_{\{\tau_C>t\}\cap\{\tau_F>t\}}]dt = \int_0^T \mathbb{E}[Z(t)\mathbb{1}_{\{\tau_C>t\}\cap\{\tau_F>t\}}]dt. \tag{14}$$

The pair of vectors $(Z, Y_{CF}) \in (\mathbb{R}^n \times B_n^1)$ is

$$Z = (Z^+(t_1) + Z^-(t_1), \ldots, Z^+(t_n) + Z^-(t_n)) \quad \textit{and} \quad Y_{CF} = (\mathbb{1}_{\{\tau_C>t_1\}\cap\{\tau_F>t_1\}}, \ldots, \mathbb{1}_{\{\tau_C>t_n\}\cap\{\tau_F>t_n\}}), \tag{15}$$

and the pair of vectors $(Z^+, Z^-) \in (\mathbb{R}_+^n \times \mathbb{R}_-^n)$ is

$$Z^+ = (f_c(t_0,t_1)X^+(t_1), \ldots, f_c(t_{n-1},t_n)X^+(t_n)) \quad \textit{and} \quad Z^- = (f_b(t_0,t_1)X^-(t_1), \ldots, f_b(t_{n-1},t_n)X^-(t_n)). \tag{16}$$

Here B_n^1 denotes the set of survival time vectors: binary vectors of ones and zeros with n components, and at most one block of ones followed by a complementary block of zeros. The empirical measure Φ_N, in terms of Dirac measure $\delta_{(z_i, y_i^{cf})}$, is

$$\Phi_N := \frac{1}{N}\sum_{i=1}^N \delta_{(z_i, y_i^{cf})}. \tag{17}$$

Under the empirical measure, Φ_N, FVA is a sum of expectations of inner products

$$FVA = \mathbb{E}^{\Phi_N}[\langle Z^+, Y_{CF}\rangle] + \mathbb{E}^{\Phi_N}[\langle Z^-, Y_{CF}\rangle] = \mathbb{E}^{\Phi_N}[\langle Z, Y_{CF}\rangle]. \tag{18}$$

In the context of this work, the ambiguity set for probability measures is

$$\mathscr{U}_{\delta_3}(\Phi_N) = \{P : D_c(\Phi, \Phi_N) \leq \delta_3\} \tag{19}$$

where D_c is the optimal transport cost or Wasserstein discrepancy for cost function c (Blanchet et al., 2018). For convenience the definition for D_c is

$$D_c(\Phi, \Phi') = \inf\{\mathbb{E}^{\pi}[c(\xi_A, \xi_B)] : \pi \in \mathscr{P}(\mathbb{R}^d \times \mathbb{R}^d), \xi_A \sim \Phi, \xi_B \sim \Phi'\} \tag{20}$$

where π belongs to the set of joint distributions with marginals Φ and Φ'. Here ξ_A denotes $(Z_A, Y_A) \in (\mathbb{R}^n \times B_n^1)$ and ξ_B denotes $(Z_B, Y_B) \in (\mathbb{R}^n \times B_n^1)$ respectively. This work uses the cost function c_{S_3} where

$$c_{S_3}((u,v),(z,y)) = S_3\langle v - y, v - y\rangle + \langle u - z, u - z\rangle. \tag{21}$$

The scale factor $S_3 > 0$ is used to compensate for different domains: $(u,v) \in (\mathbb{R}^n \times B_n^1), (z,y) \in (\mathbb{R}^n \times B_n^1)$.

2. Theory: Robust XVA and Wrong Way Risk

2.1 Unilateral CVA, DVA

The robust unilateral CVA can be written as

$$\sup_{P \in \mathscr{U}_{\delta_1}(P_N)} \mathbb{E}^P[\langle X^+, Y_C\rangle] P1. \tag{22}$$

Similarly, the robust unilateral DVA is

$$-\sup_{Q \in \mathscr{U}_{\delta_2}(Q_N)} \mathbb{E}^Q[\langle X^-, Y_F\rangle] P2. \tag{23}$$

As such, the dual formulations and solutions to the above primal optimization problems are special cases of the solutions to the bilateral CVA optimization problems, to be described next.

2.2 Bilateral CVA

2.2.1 Inner Optimization Problem

The robust bilateral CVA is

$$\sup_{\Phi \in \mathscr{U}_{\delta_3}(\Phi_N)} \mathbb{E}^{\Phi}[\langle X^+, Y_C\rangle + \langle X^-, Y_F\rangle] P3. \tag{24}$$

Similar to before, use recent duality results, noting that the inner product $\langle\,;\rangle$ satisfies the upper semicontinuous condition of the Lagrangian duality theorem, and cost function c_S satisfies the non-negative lower semicontinuous condition (see Blanchet and Murthy (2019) Assumptions 1 & 2, Gao and Kleywegt (2016)). Hence the dual problem can be written as

$$\inf_{\alpha \geq 0} F(\alpha) := \left[\alpha\delta_3 + \frac{1}{N}\sum_{i=1}^{N} \Psi_\alpha(x_i, y_i^c, y_i^f)\right] D3 \tag{25}$$

where $\Psi_\alpha(x_i, y_i^c, y_i^f) = \sup_{u \in \mathbb{R}^n, v_1 \in B_n^1, v_2 \in B_n^1}[\langle u^+, \mathbb{1}_{\{v_1 < v_2\}} v_1\rangle + \langle u^-, \mathbb{1}_{\{v_2 < v_1\}} v_2\rangle - \alpha c_{S_3}((u, v_1, v_2), (x_i, y_i^c, y_i^f))]$
$= \sup_{u \in \mathbb{R}^n, v_1 \in B_n^1, v_2 \in B_n^1}[\langle u^+, \mathbb{1}_{\{v_1 < v_2\}} v_1\rangle + \langle u^-, \mathbb{1}_{\{v_2 < v_1\}} v_2\rangle - \alpha(\langle u - x_i, u - x_i\rangle + S_3\langle v_1 - y_i^c, v_1 - y_i^c\rangle$
$+ S_3\langle v_2 - y_i^f, v_2 - y_i^f\rangle)]$.

Note that default times (v_1, v_2) are compared via the indicator function $\mathbb{1}_{\{v_1 \leqq v_2\}}$ by comparing indices (into the fixed dates array $0 < t_1 < \cdots < t_n = T$) of the respective default times. So if v_1 has a one element in index i and either $\|v_2\| = 0$ or v_2 has a one element in index j and $i < j$ then $\mathbb{1}_{\{v_1 < v_2\}} = 1$ else if $i > j$ or $\|v_1\| = 0$ then $\mathbb{1}_{\{v_1 < v_2\}} = 0$. The probability that $i = j$ for any $i, j \in \{1, \ldots, n\}$ is zero in continuous time, hence this case is not considered here. Also $\|v_1\| = 1$ implies default time $v_1 \leq t_n = T$, the maturity date of the CVA calculation. Similar analysis applies to v_2.

Now apply change of variables

$w_1 = (u - x_i)$, $w_2 = (v_1 - y_i^c)$, and $w_3 = (v_2 - y_i^f)$ to get $\Psi_\alpha(x_i, y_i^c, y_i^f) = \sup_{w_1 \in \mathbb{R}^n, w_2 \in B_n^2, w_3 \in B_n^2} \left[\langle (w_1 + x_i)^+, \mathbb{1}_{\{w_2 + y_i^c < w_3 + y_i^f\}} w_2 + y_i^c \rangle + \langle (w_1 + x_i)^-, \mathbb{1}_{\{w_3 + y_i^f < w_2 + y_i^c\}} w_3 + y_i^f \rangle - \alpha(\langle w_1, w_1 \rangle + S_3 \langle w_2, w_2 \rangle + S_3 \langle w_3, w_3 \rangle) \right]$.

It turns out that Ψ_α can be expressed as the pointwise max of four functions of more complex forms. The four functions represent the four logical cases for w_2 and w_3 each being zero or non-zero. Furthermore, we need to consider the sub-cases where the counterparty defaults before the firm, as in Ψ_α^a or vice-versa as in Ψ_α^b. Again, Ψ_α quantifies the adversarial moves in CVA and DVA across both time and spatial dimensions while accounting for the associated cost via the K terms. Please note this result involves some lengthy and tedious derivations and requires some time to go through. However, there are some patterns across the various cases and sub-cases which does simplify the analysis to some extent.

Table 1. Lookup table of optimization sub-problems

Optimization	*Objective Function*	*Solution*
$\sup_{w_1 \in \mathbb{R}^n}$	$\langle w_1, y_i \rangle - \alpha \langle w_1, w_1 \rangle$	$\frac{\|y_i\|^2}{4\alpha}$
$\sup_{w_1 \le x_{i\tau_2}}$	$\langle w_1, y_i \rangle - \alpha \langle w_1, w_1 \rangle$	$[x_{i\tau_2} \wedge \frac{\|y_i\|}{2\alpha}] - \alpha [x_{i\tau_2} \wedge \frac{\|y_i\|}{2\alpha}]^2$
$\sup_{w_1 \in \mathbb{R}^n}$	$\langle (w_1 + x_i)^+, y_i \rangle - \alpha \langle w_1, w_1 \rangle$	$[\frac{1}{4\alpha} + \langle x_i, y_i \rangle]^+$
$\sup_{w_1 \in \mathbb{R}^n}$	$\langle (w_1 + x_i)^-, y_i \rangle - \alpha \langle w_1, w_1 \rangle$	$\mathbb{1}_{\{(x_{i\tau_2} < -\frac{1}{2\alpha}) \vee (x_{i\tau_2} > 0)\}} \left[\frac{1}{4\alpha} + \langle x_i, y_i \rangle \right]^- - \mathbb{1}_{\{-\frac{1}{2\alpha} \le x_{i\tau_2} \le 0\}} \left[\alpha (\langle x_i, y_i \rangle)^2 \right]$
$\sup_{w_1 \in \mathbb{R}^n}$	$(w_1 + x_{i\tau_1})^- - \alpha \langle w_1, w_1 \rangle$	$\mathbb{1}_{\{(x_{i\tau_1} < -\frac{1}{2\alpha}) \vee (x_{i\tau_1} > 0)\}} \left[\frac{1}{4\alpha} + \langle x_i, y_i \rangle + (x_{i\tau_1} - x_{i\tau_2}) \right]^-$ $- \mathbb{1}_{\{-\frac{1}{2\alpha} \le x_{i\tau_1} \le 0\}} \left[\alpha (x_{i\tau_1})^2 \right]$

solutions are derived and used in proofs of propositions

We have $\Psi_\alpha(x_i, y_i^c, y_i^f) = \bigvee_{k=1}^4 \Psi_\alpha^k(x_i, y_i^c, y_i^f)$ where
$\Psi_\alpha^1(x_i, y_i^c, y_i^f) = \mathbb{1}_{(y_i^c < y_i^f)} \Psi_\alpha^{1a}(x_i, y_i^c, y_i^f) + \mathbb{1}_{(y_i^f < y_i^c)} \Psi_\alpha^{1b}(x_i, y_i^c, y_i^f)$,
$\Psi_\alpha^2(x_i, y_i^c, y_i^f) = \mathbb{1}_{(w_2 + y_i^c < y_i^f)} \Psi_\alpha^{2a}(x_i, y_i^c, y_i^f) + \mathbb{1}_{(y_i^f < w_2 + y_i^c)} \Psi_\alpha^{2b}(x_i, y_i^c, y_i^f)$,
$\Psi_\alpha^3(x_i, y_i^c, y_i^f) = \mathbb{1}_{(y_i^c < w_3 + y_i^f)} \Psi_\alpha^{3a}(x_i, y_i^c, y_i^f) + \mathbb{1}_{(w_3 + y_i^f < y_i^c)} \Psi_\alpha^{3b}(x_i, y_i^c, y_i^f)$,
$\Psi_\alpha^4(x_i, y_i^c, y_i^f) = \mathbb{1}_{(w_2 + y_i^c < w_3 + y_i^f)} \Psi_\alpha^{4a}(x_i, y_i^c, y_i^f) + \mathbb{1}_{(w_3 + y_i^f < w_2 + y_i^c)} \Psi_\alpha^{4b}(x_i, y_i^c, y_i^f)$,

and (suppressing arguments for brevity):
$\Psi_\alpha^{1a} = \left[\frac{1}{4\alpha} + \langle x_i, y_i^c \rangle \right]^+$, $\Psi_\alpha^{1b} = \left[\mathbb{1}_{\{(x_{i\tau_2} < -\frac{1}{2\alpha}) \vee (x_{i\tau_2} > 0)\}} \left[\frac{1}{4\alpha} + \langle x_i, y_i^f \rangle \right]^- - \mathbb{1}_{\{-\frac{1}{2\alpha} \le x_{i\tau_2} \le 0\}} \left[\alpha (\langle x_i, y_i^f \rangle)^2 \right] \right]$,
$\Psi^{2a} = \left[\left[\frac{1}{4\alpha} + \langle x_i, y_i^c \rangle + (x_{i\tau_1^*} - x_{i\tau_2}) \right]^+ - \alpha S_3 K^{2a} \right]$, $\Psi_\alpha^{2b} = \left[\Psi_\alpha^{1b} - \alpha S_3 K^{2b} \right]$,
$\Psi^{3a} = \left[\Psi_\alpha^{1a} - \alpha S_3 K^{3a} \right]$, $\Psi^{3b} = \left[\mathbb{1}_{\{(x_{i\tau_1^*} < -\frac{1}{2\alpha}) \vee (x_{i\tau_1^*} > 0)\}} \left[\frac{1}{4\alpha} + \langle x_i, y_i^f \rangle + (x_{i\tau_1^*} - x_{i\tau_2}) \right]^- - \mathbb{1}_{\{-\frac{1}{2\alpha} \le x_{i\tau_1^*} \le 0\}} \left[\alpha (x_{i\tau_1^*})^2 \right] - \alpha S_3 K^{3b} \right]$,
$\Psi^{4a} = \left[\Psi^{2a} - \alpha S_3 (K^{4a} - K^{2a}) \right]$, $\Psi^{4b} = \left[\Psi^{3b} - \alpha S_3 (K^{4b} - K^{3b}) \right]$.

Note parameter τ_1^* and constant K are defined within the proof by **cases** (see Supplementary Material), and are omitted here for brevity. Recall τ_2 is index τ such that $y_{i\tau}^{\{c,f\}} = 1$ else it is 0 if $\|y_i^{\{c,f\}}\| = 0$. The selection in $\{c, f\}$ is determined by context. This result follows from jointly maximizing the adversarial exposure w_1 and the default time indices w_2, w_3. The structure of B_n^2 allows us to decouple this joint maximization and find the critical point to maximize the quadratic in w_1 and write down the condition to select the optimal default time index τ_1^* for either the counterparty (in sub-case a) or the firm (in sub-case b), as determined by first to default. Finally, take the max over the four logical cases for w_2 and w_3 to arrive at the solution. The K terms represent the cost associated with the worst case BCVA.

The particular structure of B_n^1 and B_n^2 will be exploited to evaluate the sup above. The analysis proceeds by considering different cases for optimal values (w_1^*, w_2^*, w_3^*).

Case 1 Suppose $w_2^* = 0, w_3^* = 0$. Then

$$\Psi_\alpha(x_i,y_i^c,y_i^f)=\sup_{w_1\in\mathbb{R}^n}\left[\langle(w_1+x_i)^+,\mathbb{1}_{\{y_i^c<y_i^f\}}y_i^c\rangle+\langle(w_1+x_i)^-,\mathbb{1}_{\{y_i^f<y_i^c\}}y_i^f\rangle-\alpha(\langle w_1,w_1\rangle)\right]. \tag{26}$$

a) Suppose $\mathbb{1}_{(y_i^c<y_i^f)}=1$. Then

$$\Psi_\alpha(x_i,y_i^c,y_i^f)=\sup_{w_1\in\mathbb{R}^n}\left[\langle(w_1+x_i)^+,y_i^c\rangle-\alpha(\langle w_1,w_1\rangle)\right]. \tag{27}$$

Therefore $\|y_i^c\|=1$. Let τ_2 denote default time for y_i^c. Simplify further to get

$$\Psi_\alpha(x_i,y_i^c,y_i^f)=\sup_{w_{1\tau_2}\in\mathbb{R}}\left[(w_{1\tau_2}+x_{i\tau_2})^+-\alpha(w_{1\tau_2})^2\right]. \tag{28}$$

Now follow the approach in Bartl et al. (2017) to write down the first order optimality condition:

$$\mathbb{1}_{(0,\infty)}(w_{1\tau_2}+x_{i\tau_2})-2\alpha w_{1\tau_2}\geq 0\geq\mathbb{1}_{[0,\infty)}(w_{1\tau_2}+x_{i\tau_2})-2\alpha w_{1\tau_2}. \tag{29}$$

i) Suppose $(w^*_{1\tau_2}+x_{i\tau_2})<0$. Then $w^*_{1\tau_2}=0$. So $x_{i\tau_2}<0 w^*_{i\tau_2}=0$.

ii) Suppose $(w^*_{1\tau_2}+x_{i\tau_2})>0$. Then $w^*_{1\tau_2}=\frac{1}{2\alpha}$. So $x_{i\tau_2}>-\frac{1}{2\alpha}w^*_{1\tau_2}=\frac{1}{2\alpha}$.

iii) Note $(w^*_{1\tau_2}+x_{i\tau_2})=0$ is not possible (does not satisfy first order optimality condition).

Considering the intervals for $x_{i\tau_2}$ above, there are three cases as below.

i) $x_{i\tau_2}\geq 0 w^*_{1\tau_2}=\frac{1}{2\alpha}\Psi_\alpha=[\frac{1}{4\alpha}+x_{i\tau_2}]$.

ii) $x_{i\tau_2}\leq-\frac{1}{2\alpha}w^*_{1\tau_2}=0\Psi_\alpha=0$.

iii) $(-\frac{1}{2\alpha}<x_{i\tau_2}<0)\Psi_\alpha=[\frac{1}{4\alpha}+x_{i\tau_2}]^+$.

In summary, considering all cases above, conclude that

$$\Psi^{1a}_\alpha(x_i,y_i^c,y_i^f)=\left[\frac{1}{4\alpha}+x_{i\tau_2}\right]^+. \tag{30}$$

This can also be expressed as

$$\Psi^{1a}_\alpha(x_i,y_i^c,y_i^f)=\left[\frac{1}{4\alpha}+\langle x_i,y_i^c\rangle\right]^+. \tag{31}$$

b) Suppose $\mathbb{1}_{(y_i^f<y_i^c)}=1$. Then

$$\Psi_\alpha(x_i,y_i^c,y_i^f)=\sup_{w_1\in\mathbb{R}^n}\left[\langle(w_1+x_i)^-,y_i^f\rangle-\alpha(\langle w_1,w_1\rangle)\right]. \tag{32}$$

Therefore $\|y_i^f\|=1$. Let τ_2 denote default time for y_i^f. Simplify further to get

$$\Psi_\alpha(x_i,y_i^c,y_i^f)=\sup_{w_{1\tau_2}\in\mathbb{R}}\left[(w_{1\tau_2}+x_{i\tau_2})^--\alpha(w_{1\tau_2})^2\right]. \tag{33}$$

Now follow the approach in Bartl et al. (2017) to write down the first order optimality condition:

$$\mathbb{1}_{(-\infty,0]}(w_{1\tau_2}+x_{i\tau_2})-2\alpha w_{1\tau_2}\geq 0\geq\mathbb{1}_{(-\infty,0)}(w_{1\tau_2}+x_{i\tau_2})-2\alpha w_{1\tau_2}. \tag{34}$$

i) Suppose $(w^*_{1\tau_2}+x_{i\tau_2})>0$. Then $w^*_{1\tau_2}=0$. So $x_{i\tau_2}>0 w^*_{1\tau_2}=0$.

ii) Suppose $(w^*_{1\tau_2}+x_{i\tau_2})<0$. Then $w^*_{1\tau_2}=\frac{1}{2\alpha}$. So $x_{i\tau_2}<-\frac{1}{2\alpha}w^*_{1\tau_2}=\frac{1}{2\alpha}$.

iii) Note $(w^*_{1\tau_2}+x_{i\tau_2})=0$ is not possible (does not satisfy first order optimality condition).

Considering the intervals for $x_{i\tau_2}$ above, there are three cases as below.

i) $x_{i\tau_2}>0 w^*_{1\tau_2}=0\Psi_\alpha=0$.

ii) $x_{i\tau_2} < -\frac{1}{2\alpha} w^*_{i\tau_2} = \frac{1}{2\alpha}\Psi_\alpha = [\frac{1}{4\alpha} + x_{i\tau_2}]$.

iii) $[-\frac{1}{2\alpha} \le x_{i\tau_2} \le 0] w^*_{1\tau_2} = |x_{i\tau_2}|$.
Note the slope $(1 - 2\alpha w_{1\tau_2})$ is positive for $0 \le w_{1\tau_2} < \frac{1}{2\alpha}$, and equals zero at $w_{1\tau_2} = \frac{1}{2\alpha}$.
However, $(w_{1\tau_2} + x_{i\tau_2})^-$ attains its max value of zero for $w_{i\tau_2} = |x_{i\tau_2}|$ so stop there.

In summary, considering all cases above, conclude that

$$\Psi^{1b}_\alpha(x_i, y^c_i, y^f_i) = \left[\mathbb{1}_{\{(x_{i\tau_2} < -\frac{1}{2\alpha}) \vee (x_{i\tau_2} > 0)\}} \big[\frac{1}{4\alpha} + x_{i\tau_2}\big]^- - \mathbb{1}_{\{-\frac{1}{2\alpha} \le x_{i\tau_2} \le 0\}} \big[\alpha (x_{i\tau_2})^2\big] \right]. \tag{35}$$

This can also be expressed as

$$\Psi^{1b}_\alpha(x_i, y^c_i, y^f_i) = \left[\mathbb{1}_{\{(x_{i\tau_2} < -\frac{1}{2\alpha}) \vee (x_{i\tau_2} > 0)\}} \big[\frac{1}{4\alpha} + \langle x_i, y^f_i \rangle\big]^- - \mathbb{1}_{\{-\frac{1}{2\alpha} \le x_{i\tau_2} \le 0\}} \big[\alpha (\langle x_i, y^f_i \rangle)^2\big] \right]. \tag{36}$$

c) Suppose $\mathbb{1}_{(\|y^f_i\| = \|y^c_i\| = 0)} = 1$.
In this trivial case, $\Psi_\alpha = 0$. Note there is no third subcase for $Cases 2-4$ below since that would imply $w^*_2 = 0, w^*_3 = 0$.

Finally, to sum up Case 1, considering parts a) and b), let us write:

$$\Psi^1_\alpha(x_i, y^c_i, y^f_i) = \mathbb{1}_{(y^c_i < y^f_i)} \Psi^{1a}_\alpha(x_i, y^c_i, y^f_i) + \mathbb{1}_{(y^f_i < y^c_i)} \Psi^{1b}_\alpha(x_i, y^c_i, y^f_i). \tag{37}$$

Case 2 Suppose $w^*_2 \neq 0, w^*_3 = 0$.
Then w^*_2 has +1 in position τ^*_1 and -1 in position τ_2, where $\tau_j = 0$ means the value ± 1 does not occur.
Furthermore, $\tau^*_1 \neq \tau_2$ otherwise $w^*_2 = 0$.

$$\Psi_\alpha(x_i, y^c_i, y^f_i) = \sup_{w_1 \in \mathbb{R}^n, w_2 \in B^2_n} \big[\langle (w_1 + x_i)^+, \mathbb{1}_{\{w_2 + y^c_i < y^f_i\}} w_2 + y^c_i \rangle + \langle (w_1 + x_i)^-, \mathbb{1}_{\{y^f_i < w_2 + y^c_i\}} y^f_i \rangle - \alpha(\langle w_1, w_1 \rangle + S_3 \langle w_2, w_2 \rangle) \big]. \tag{38}$$

a) Suppose $\mathbb{1}_{(w_2 + y^c_i < y^f_i)} = 1$. Then

$$\Psi_\alpha(x_i, y^c_i, y^f_i) = \sup_{w_1 \in \mathbb{R}^n, w_2 \in B^2_n} \big[\langle (w_1 + x_i)^+, w_2 + y^c_i \rangle - \alpha(\langle w_1, w_1 \rangle + S_3 \langle w_2, w_2 \rangle) \big]. \tag{39}$$

Recall $\langle (w_1 + x_i), (w_2 + y^c_i) \rangle = (w_{1\tau_1} + x_{i\tau_1})$. Also recall τ_1 and τ_2 are associated with y^c_i. Let $\tau_{2,f}$ denote default time (index) for y^f_i. The default time constraint implies $\tau_1 < \tau_{2,f}$. Therefore $\tau_1 > 0$. The structure of finite set B^2_n implies

$$\Psi_\alpha(x_i, y^c_i, y^f_i) = \sup_{w_1 \in \mathbb{R}^n, 0 < \tau_1 < \tau_{2,f}, \tau_1 \neq \tau_2} \big[(w_{1\tau_1} + x_{i\tau_1})^+ - \alpha(\langle w_1, w_1 \rangle + S_3 \langle w_2, w_2 \rangle) \big]. \tag{40}$$

Observe the only positive component for $w_1 \in \mathbb{R}^n$ in sup above is τ_1.

$$\sup_{w_1 \in \mathbb{R}^n} \big[(w_{1\tau_1} + x_{i\tau_1})^+ - \alpha \langle w_1, w_1 \rangle \big] = \sup_{w_{1\tau_1} \in \mathbb{R}} \big[(w_{1\tau_1} + x_{i\tau_1})^+ - \alpha (w^2_{1\tau_1}) \big]. \tag{41}$$

Evaluating at the critical point $w^*_{1\tau_1} = \frac{1}{2\alpha} \in \mathbb{R}$ for the above quadratic gives

$$\sup_{w_{1\tau_1} \in \mathbb{R}} \big[(w_{1\tau_1} + x_{i\tau_1})^+ - \alpha (w^2_{1\tau_1}) \big] = \big[\frac{1}{4\alpha} + x_{i\tau_1} \big]^+. \tag{42}$$

Therefore one can write

$$\Psi_\alpha(x_i, y^c_i, y^f_i) = \max_{0 < \tau_1 < \tau_{2,f}, \tau_1 \neq \tau_2} \big[\frac{1}{4\alpha} + x_{i\tau_1} \big]^+ - \alpha S_3 K^{2a} \tag{43}$$

where $K^{2a} := (1 + \mathbb{1}_{\{\tau_2 \neq 0\}})$. Furthermore, τ^*_1 is determined as

$$\tau^*_1 = \max_{0 < \tau_1 < \tau_{2,f}, \tau_1 \neq \tau_2} [x^+_{i\tau_1}]. \tag{44}$$

Substituting back into expression for Ψ_α gives

$$\Psi_\alpha^{2a}(x_i, y_i^c, y_i^f) = \left[\left[\frac{1}{4\alpha} + x_{i\tau_1^*} \right]^+ - \alpha S_3 K^{2a} \right]. \tag{45}$$

This can also be expressed as

$$\Psi_\alpha^{2a}(x_i, y_i^c, y_i^f) = \left[\left[\frac{1}{4\alpha} + \langle x_i, y_i^c \rangle + (x_{i\tau_1^*} - x_{i\tau_2}) \right]^+ - \alpha S_3 K^{2a} \right]. \tag{46}$$

b) Suppose $\mathbb{1}_{(y_i^f < w_2 + y_i^c)} = 1$. Then

$$\Psi_\alpha(x_i, y_i^c, y_i^f) = \sup_{w_1 \in \mathbb{R}^n, w_2 \in B_n^2} \left[\langle (w_1 + x_i)^-, y_i^f \rangle - \alpha(\langle w_1, w_1 \rangle + S_3 \langle w_2, w_2 \rangle) \right]. \tag{47}$$

Recall τ_1 and τ_2 are associated with y_i^c. Let $\tau_{2,f}$ denote the default time (index) for y_i^f. The default time constraint implies $\tau_{2,f} < \tau_1$. Therefore $\tau_{2,f} > 0$ and $\|y_i^f\| = 1$. Note the only non-zero component of $\|y_i^f\|$ is $\tau_{2,f}$. Hence set $w_{1\tau}^* = 0 \, \forall \tau \neq \tau_{2,f}$. Simplifying further

$$\Psi_\alpha(x_i, y_i^c, y_i^f) = \sup_{w_{1\tau_{2,f}} \in \mathbb{R}, w_2 \in B_n^2} \left[(w_{1\tau_{2,f}} + x_{i\tau_{2,f}})^- - \alpha((w_{1\tau_{2,f}})^2 + S_3 K^{2b}) \right]. \tag{48}$$

where $K^{2b} := (\mathbb{1}_{\{\tau_1 \neq 0\}} + \mathbb{1}_{\{\tau_2 \neq 0\}}) = 1$. For K^{2b}, if $\tau_2 = 0$, then $\tau_1 \neq 0$ since $w_2^* \neq 0$. Otherwise set $\tau_1 = 0$ if $\tau_2 \neq 0$ to maximize $\sup_{w_2}$ above. Following the calculations in *Case* 1*b*) above, conclude that

$$\Psi_\alpha^{2b}(x_i, y_i^c, y_i^f) = \left[\mathbb{1}_{\{(x_{i\tau_2} < -\frac{1}{2\alpha}) \vee (x_{i\tau_2} > 0)\}} \left[\frac{1}{4\alpha} + x_{i\tau_2} \right]^- - \mathbb{1}_{\{-\frac{1}{2\alpha} \leq x_{i\tau_2} \leq 0\}} \left[\alpha (x_{i\tau_2})^2 \right] - \alpha S_3 K^{2b} \right]. \tag{49}$$

This can also be expressed as

$$\Psi_\alpha^{2b}(x_i, y_i^c, y_i^f) = \left[\mathbb{1}_{\{(x_{i\tau_2} < -\frac{1}{2\alpha}) \vee (x_{i\tau_2} > 0)\}} \left[\frac{1}{4\alpha} + \langle x_i, y_i^f \rangle \right]^- - \mathbb{1}_{\{-\frac{1}{2\alpha} \leq x_{i\tau_2} \leq 0\}} \left[\alpha (\langle x_i, y_i^f \rangle)^2 \right] - \alpha S_3 K^{2b} \right]. \tag{50}$$

Finally, to sum up Case 2, considering parts a) and b), let us write:

$$\Psi_\alpha^2(x_i, y_i^c, y_i^f) = \mathbb{1}_{(w_2 + y_i^c < y_i^f)} \Psi_\alpha^{2a}(x_i, y_i^c, y_i^f) + \mathbb{1}_{(y_i^f < w_2 + y_i^c)} \Psi_\alpha^{2b}(x_i, y_i^c, y_i^f). \tag{51}$$

Case 3 Suppose $w_2^* = 0, w_3^* \neq 0$.
Then w_3^* has +1 in position τ_1^* and -1 in position τ_2, where $\tau_j = 0$ means the value ± 1 does not occur.
Furthermore, $\tau_1^* \neq \tau_2$ otherwise $w_3^* = 0$.

$$\Psi_\alpha(x_i, y_i^c, y_i^f) = \sup_{w_1 \in \mathbb{R}^n, w_3 \in B_n^2} \left[\langle (w_1 + x_i)^+, \mathbb{1}_{\{y_i^c < w_3 + y_i^f\}} y_i^c \rangle + \langle (w_1 + x_i)^-, \mathbb{1}_{\{w_3 + y_i^f < y_i^c\}} w_3 + y_i^f \rangle - \alpha(\langle w_1, w_1 \rangle + S_3 \langle w_3, w_3 \rangle) \right]. \tag{52}$$

a) Suppose $\mathbb{1}_{(y_i^c < w_3 + y_i^f)} = 1$. Then

$$\Psi_\alpha(x_i, y_i^c, y_i^f) = \sup_{w_1 \in \mathbb{R}^n, w_3 \in B_n^2} \left[\langle (w_1 + x_i)^+, y_i^c \rangle - \alpha(\langle w_1, w_1 \rangle + S_3 \langle w_3, w_3 \rangle) \right]. \tag{53}$$

Recall $\langle (w_1 + x_i), y_i^c \rangle = (w_{1\tau_2} + x_{i\tau_2})$. Also recall τ_1 and τ_2 are associated with y_i^f. Let $\tau_{2,c}$ denote the default time (index) for y_i^c. The default time constraint implies $\tau_{2,c} < \tau_1$. Therefore $\tau_{2,c} > 0$ and $\|y_i^c\| = 1$. Note the only positive component of $\|y_i^c\|$ is $\tau_{2,c}$. Hence set $w_{1\tau}^* = 0 \, \forall \tau \neq \tau_{2,c}$. Simplify further to get

$$\Psi_\alpha(x_i, y_i^c, y_i^f) = \sup_{w_{1\tau_{2,c}} \in \mathbb{R}, w_3 \in B_n^2} \left[(w_{1\tau_{2,c}} + x_{i\tau_{2,c}})^+ - \alpha((w_{1\tau_{2,c}})^2 + S_3 K^{3a}) \right] \tag{54}$$

where $K^{3a} := (\mathbb{1}_{\{\tau_1 \neq 0\}} + \mathbb{1}_{\{\tau_2 \neq 0\}}) = 1$, following logic in Case 2b) above. Evaluating at the critical point $w_{1\tau_{2,c}}^* =$

$\frac{1}{2\alpha} \in \mathbb{R}$ gives

$$\sup_{w_{1\tau_{2,c}} \in \mathbb{R}} \left[(w_{1\tau_{2,c}} + x_{i\tau_{2,c}})^+ - \alpha(w_{1\tau_{2,c}}^2) \right] = \left[\frac{1}{4\alpha} + x_{i\tau_{2,c}} \right]^+. \tag{55}$$

Therefore one can write

$$\Psi_\alpha(x_i, y_i^c, y_i^f) = \left[\frac{1}{4\alpha} + x_{i\tau_{2,c}} \right]^+ - \alpha S_3 K^{3a}. \tag{56}$$

This can also be expressed as

$$\Psi_\alpha^{3a}(x_i, y_i^c, y_i^f) = \left[\left[\frac{1}{4\alpha} + \langle x_i, y_i^c \rangle \right]^+ - \alpha S_3 K^{3a} \right]. \tag{57}$$

b) Suppose $\mathbb{1}_{(w_3 + y_i^f < y_i^c)} = 1$. Then

$$\Psi_\alpha(x_i, y_i^c, y_i^f) = \sup_{w_1 \in \mathbb{R}^n, w_3 \in B_n^2} \left[\langle (w_1 + x_i)^-, w_3 + y_i^f \rangle - \alpha(\langle w_1, w_1 \rangle + S_3 \langle w_3, w_3 \rangle) \right]. \tag{58}$$

Recall $\langle (w_1 + x_i), (w_3 + y_i^f) \rangle = (w_{1\tau_1} + x_{i\tau_1})$. Also recall τ_1 and τ_2 are associated with y_i^f. Let $\tau_{2,c}$ denote default time (index) for y_i^c. The default time constraint implies $\tau_1 < \tau_{2,c}$. Therefore $\tau_1 > 0$ and

$$\Psi_\alpha(x_i, y_i^c, y_i^f) = \sup_{w_1 \in \mathbb{R}^n, 0 < \tau_1 < \tau_{2,c}, \tau_1 \neq \tau_2} \left[(w_{1\tau_1} + x_{i\tau_1})^- - \alpha((w_{1\tau_1})^2 + S_3 K^{3b}) \right] \tag{59}$$

where $K^{3b} := (1 + \mathbb{1}_{\{\tau_2 \neq 0\}})$. Following the calculations in *Case* $2b$) above, conclude that

$$\Psi_\alpha(x_i, y_i^c, y_i^f) = \left[\mathbb{1}_{\{(x_{i\tau_1^*} < -\frac{1}{2\alpha}) \vee (x_{i\tau_1^*} > 0)\}} \left[\frac{1}{4\alpha} + x_{i\tau_1^*} \right]^- - \mathbb{1}_{\{-\frac{1}{2\alpha} \leq x_{i\tau_1^*} \leq 0\}} \left[\alpha(x_{i\tau_1^*})^2 \right] - \alpha S_3 K^{3b} \right]. \tag{60}$$

Furthermore, τ_1^* is determined as

$$\tau_1^* = {}_{0 < \tau_1 < \tau_2^c, \tau_1 \neq \tau_2} \left[x_{i\tau_1} \right]. \tag{61}$$

Therefore one can write

$$\Psi_\alpha^{3b}(x_i, y_i^c, y_i^f) = \left[\mathbb{1}_{\{(x_{i\tau_1^*} < -\frac{1}{2\alpha}) \vee (x_{i\tau_1^*} > 0)\}} \left[\frac{1}{4\alpha} + x_{i\tau_1^*} \right]^- - \mathbb{1}_{\{-\frac{1}{2\alpha} \leq x_{i\tau_1^*} \leq 0\}} \left[\alpha(x_{i\tau_1^*})^2 \right] - \alpha S_3 K^{3b} \right]. \tag{62}$$

This can also be expressed as

$$\Psi_\alpha^{3b}(x_i, y_i^c, y_i^f) = \left[\mathbb{1}_{\{(x_{i\tau_1^*} < -\frac{1}{2\alpha}) \vee (x_{i\tau_1^*} > 0)\}} \left[\frac{1}{4\alpha} + \langle x_i, y_i^f \rangle + (x_{i\tau_1^*} - x_{i\tau_2}) \right]^- - \mathbb{1}_{\{-\frac{1}{2\alpha} \leq x_{i\tau_1^*} \leq 0\}} \left[\alpha(x_{i\tau_1^*})^2 \right] - \alpha S_3 K^{3b} \right]. \tag{63}$$

Finally, to sum up Case 3, considering parts a) and b), let us write:

$$\Psi_\alpha^3(x_i, y_i^c, y_i^f) = \mathbb{1}_{(y_i^c < w_3 + y_i^f)} \Psi_\alpha^{3a}(x_i, y_i^c, y_i^f) + \mathbb{1}_{(w_3 + y_i^f < y_i^c)} \Psi_\alpha^{3b}(x_i, y_i^c, y_i^f). \tag{64}$$

Case 4 Suppose $w_2^* \neq 0, w_3^* \neq 0$.
Then w_2^* has +1 in position $\tau_{1,c}^*$ and -1 in position $\tau_{2,c}$, where $\tau_{j,c} = 0$ means the value ± 1 does not occur.
Furthermore, $\tau_{1,c}^* \neq \tau_{2,c}$ otherwise $w_2^* = 0$.
And w_3^* has +1 in position $\tau_{1,f}^*$ and -1 in position $\tau_{2,f}$, where $\tau_{j,f} = 0$ means the value ± 1 does not occur.
Furthermore, $\tau_{1,f}^* \neq \tau_{2,f}$ otherwise $w_3^* = 0$.

$\Psi_\alpha(x_i, y_i^c, y_i^f) = \sup_{w_1 \in \mathbb{R}^n, w_2 \in B_n^2, w_3 \in B_n^2} \Big[\langle (w_1 + x_i)^+, \mathbb{1}_{\{w_2 + y_i^c < w_3 + y_i^f\}} w_2 + y_i^c \rangle + \langle (w_1 + x_i)^-, \mathbb{1}_{\{w_3 + y_i^f < w_2 + y_i^c\}} w_3 + y_i^f \rangle - \alpha(\langle w_1, w_1 \rangle + S_3 \langle w_2, w_2 \rangle + S_3 \langle w_3, w_3 \rangle) \Big]$.

a) Suppose $\mathbb{1}_{(w_2+y_i^c<w_3+y_i^f)}=1$. Then

$$\Psi_\alpha(x_i,y_i^c,y_i^f)=\sup_{w_1\in\mathbb{R}^n,w_2\in B_n^2,w_3\in B_n^2}\big[\langle(w_1+x_i)^+,w_2+y_i^c\rangle-\alpha(\langle w_1,w_1\rangle+S_3\langle w_2,w_2\rangle+S_3\langle w_3,w_3\rangle)\big]. \tag{65}$$

Recall $\langle(w_1+x_i),(w_2+y_i^c)\rangle=(w_{1\tau_{1,c}}+x_{i\tau_{1,c}})$. The default time constraint implies $\tau_{1,c}<\tau_{1,f}$. Therefore $\tau_{1,c}>0$. The structure of finite set B_n^2 implies

$$\Psi_\alpha(x_i,y_i^c,y_i^f)=\sup_{w_1\in\mathbb{R}^n,0<\tau_{1,c}<\tau_{1,f},\tau_{1,c}\neq\tau_{2,c}}\big[(w_{1\tau_{1,c}}+x_{i\tau_{1,c}})^+-\alpha(\langle w_1,w_1\rangle+S_3\langle w_2,w_2\rangle+S_3\langle w_3,w_3\rangle)\big]. \tag{66}$$

Observe the only positive component for $w_1\in\mathbb{R}^n$ in sup above is $\tau_{1,c}$.

$$\sup_{w_1\in\mathbb{R}^n}\big[(w_{1\tau_{1,c}}+x_{i\tau_{1,c}})^+-\alpha\langle w_1,w_1\rangle\big]=\sup_{w_{1\tau_{1,c}}\in\mathbb{R}}\big[(w_{1\tau_{1,c}}+x_{i\tau_{1,c}})^+-\alpha(w_{1\tau_{1,c}}^2)\big]. \tag{67}$$

Evaluating at the critical point $w_{1\tau_{1,c}}^*=\frac{1}{2\alpha}\in\mathbb{R}$ for the above quadratic gives

$$\sup_{w_{1\tau_{1,c}}\in\mathbb{R}}\big[(w_{1\tau_{1,c}}+x_{i\tau_{1,c}})^+-\alpha(w_{1\tau_{1,c}}^2)\big]=\big[\frac{1}{4\alpha}+x_{i\tau_{1,c}}\big]^+. \tag{68}$$

Therefore one can write

$$\Psi_\alpha(x_i,y_i^c,y_i^f)=\max_{0<\tau_{1,c}<\tau_{1,f},\tau_{1,c}\neq\tau_{2,c}}\big[\frac{1}{4\alpha}+x_{i\tau_{1,c}}\big]^+-\alpha S_3K^{4a}. \tag{69}$$

where $K^{4a}:=(\mathbb{1}_{\{\tau_{1,c}\neq0\}}+\mathbb{1}_{\{\tau_{2,c}\neq0\}}+\mathbb{1}_{\{\tau_{1,f}\neq0\}}+\mathbb{1}_{\{\tau_{2,f}\neq0\}})=(2+\mathbb{1}_{\{\tau_{2,c}\neq0\}})$ following logic as in Case 3a) above. Furthermore, τ_1^* is determined as

$$\tau_1^*=_{0<\tau_{1,c}<\tau_{1,f},\tau_{1,c}\neq\tau_{2,c}}[x_{i\tau_{1,c}}^+]. \tag{70}$$

Substituting back into expression for Ψ_α gives

$$\Psi_\alpha^{4a}(x_i,y_i^c,y_i^f)=\Big[\big[\frac{1}{4\alpha}+x_{i\tau_1^*}\big]^+-\alpha S_3K^{4a}\Big]. \tag{71}$$

Let $\tau_2=\tau_{2,c}$. Then this can also be expressed as

$$\Psi_\alpha^{4a}(x_i,y_i^c,y_i^f)=\Big[\big[\frac{1}{4\alpha}+\langle x_i,y_i^c\rangle+(x_{i\tau_1^*}-x_{i\tau_2})\big]^+-\alpha S_3K^{4a}\Big]. \tag{72}$$

b) Suppose $\mathbb{1}_{(w_3+y_i^f<w_2+y_i^c)}=1$. Then

$$\Psi_\alpha(x_i,y_i^c,y_i^f)=\sup_{w_1\in\mathbb{R}^n,w_2\in B_n^2,w_3\in B_n^2}\big[\langle(w_1+x_i)^-,w_3+y_i^f\rangle-\alpha(\langle w_1,w_1\rangle+S_3\langle w_2,w_2\rangle+S_3\langle w_3,w_3\rangle)\big]. \tag{73}$$

Recall $\langle(w_1+x_i),(w_3+y_i^f)\rangle=(w_{1\tau_{1,f}}+x_{i\tau_{1,f}})$. The default time constraint implies $\tau_{1,f}<\tau_{1,c}$. Therefore $\tau_{1,f}>0$. The structure of finite set B_n^2 implies

$$\Psi_\alpha(x_i,y_i^c,y_i^f)=\sup_{w_1\in\mathbb{R}^n,0<\tau_{1,f}<\tau_{1,c},\tau_{1,f}\neq\tau_{2,f}}\big[(w_{1\tau_{1,f}}+x_{i\tau_{1,f}})^--\alpha(\langle w_1,w_1\rangle+S_3\langle w_2,w_2\rangle+S_3\langle w_3,w_3\rangle)\big]. \tag{74}$$

$$\Psi_\alpha(x_i,y_i^c,y_i^f)=\sup_{w_1\in\mathbb{R}^n,0<\tau_{1,f}<\tau_{1,c},\tau_{1,f}\neq\tau_{2,f}}\big[(w_{1\tau_{1,f}}+x_{i\tau_{1,f}})^--\alpha((w_{1\tau_{1,f}})^2+S_3K)\big]. \tag{75}$$

where $K:=(\mathbb{1}_{\{\tau_{1,c}\neq0\}}+\mathbb{1}_{\{\tau_{2,c}\neq0\}}+\mathbb{1}_{\{\tau_{1,f}\neq0\}}+\mathbb{1}_{\{\tau_{2,f}\neq0\}})=(2+\mathbb{1}_{\{\tau_{2,f}\neq0\}})$ following logic as in Case 4a) above. Following the calculations in *Case* 3*b*) above, conclude that

$$\Psi_\alpha(x_i,y_i^c,y_i^f)=\Big[\mathbb{1}_{\{(x_{i\tau_1^*}<-\frac{1}{2\alpha})\vee(x_{i\tau_1^*}>0)\}}\big[\frac{1}{4\alpha}+x_{i\tau_1^*}\big]^--\mathbb{1}_{\{-\frac{1}{2\alpha}\leq x_{i\tau_1^*}\leq0\}}\big[\alpha(x_{i\tau_1^*})^2\big]-\alpha S_3K\Big]. \tag{76}$$

Furthermore, τ_1^* is determined as

$$\tau_1^* = {}_{0<\tau_{1,f}<\tau_{1,c},\tau_{1,f}\neq\tau_{2,f}}\left[x_i\tau_{1,f}\right]. \tag{77}$$

Therefore one can write

$$\Psi_\alpha^{4b}(x_i,y_i^c,y_i^f) = \left[\mathbb{1}_{\{(x_{i\tau_1^*}<-\frac{1}{2\alpha})\vee(x_{i\tau_1^*}>0)\}}\left[\frac{1}{4\alpha}+x_{i\tau_1^*}\right]^- - \mathbb{1}_{\{-\frac{1}{2\alpha}\leq x_{i\tau_1^*}\leq 0\}}\left[\alpha(x_{i\tau_1^*})^2\right]-\alpha S_3K^{4b}\right]. \tag{78}$$

Let $\tau_2=\tau_{2,f}$. Then this can also be expressed as

$$\Psi_\alpha^{4b}(x_i,y_i^c,y_i^f) = \left[\mathbb{1}_{\{(x_{i\tau_1^*}<-\frac{1}{2\alpha})\vee(x_{i\tau_1^*}>0)\}}\left[\frac{1}{4\alpha}+\langle x_i,y_i^f\rangle+(x_{i\tau_1^*}-x_{i\tau_2})\right]^- - \mathbb{1}_{\{-\frac{1}{2\alpha}\leq x_{i\tau_1^*}\leq 0\}}\left[\alpha(x_{i\tau_1^*})^2\right]-\alpha S_3K^{4b}\right]. \tag{79}$$

Finally, to sum up Case 4, considering parts a) and b), let us write:

$$\Psi_\alpha^4(x_i,y_i^c,y_i^f) = \mathbb{1}_{(w_2+y_i^c<w_3+y_i^f)}\Psi_\alpha^{4a}(x_i,y_i^c,y_i^f)+\mathbb{1}_{(w_3+y_i^f<w_2+y_i^c)}\Psi_\alpha^{4b}(x_i,y_i^c,y_i^f). \tag{80}$$

2.2.2 Outer Optimization Problem

The goal now is to evaluate

$$\inf_{\alpha\geq 0} F(\alpha) := \left[\alpha\delta_3+\frac{1}{N}\sum_{i=1}^N\Psi_\alpha(x_i,y_i^c,y_i^f)\right] \tag{81}$$

where the Ψ_α functions are given as the solutions to Proposition 2.1. Although Lagrangian duality implies the convexity of $F(\alpha)$, due to its complexity, computational methods and solvers are used to evaluate this expression. Nonetheless, the solution can be expressed as below. Note that for $\delta_3=0$ one recovers the expression for original CVA^{B} given in Section 1.3.3.

The primal problem 24 has solution $\left[\alpha^*\delta_3+\frac{1}{N}\sum_{i=1}^N\Psi_{\alpha^*}(x_i,y_i^c,y_i^f)\right]$
where $\alpha^* = {}_{\alpha\geq 0}\left[\alpha\delta_3+\frac{1}{N}\sum_{i=1}^N\Psi_\alpha(x_i,y_i^c,y_i^f)\right]$ and $\Psi_{\alpha^*}(x_i,y_i^c,y_i^f)=\bigvee_{k=1}^4\Psi_{\alpha^*}^k(x_i,y_i^c,y_i^f)$.
Expressed in terms of original BCVA, this says

$$\sup_{\Phi\in\mathscr{U}_{\delta_3}(\Phi_N)}\mathbb{E}^\Phi[\langle X^+,Y^C\rangle+\langle X^-,Y^F\rangle] = \mathbb{E}^{P_N}[\langle X^+,Y^C\rangle+\langle X^-,Y^F\rangle]+\alpha^*\delta_3+\mathbb{E}^{P_N}\left[\Psi_{\alpha^*}(X,Y^C,Y^F)-[\langle X^+,Y^C\rangle+\langle X^-,Y^F\rangle]\right]^+ \tag{82}$$

where the additional terms represent a penalty due to ambiguity in probability distribution. This follows directly from the previous proposition. $\delta_3=0$ reduces to original BCVA. This follows by direct substitution of α^* as characterized above into the dual problem 25.

2.2.3 Recovering the Worst Case Distribution

The process of recovering the worst case CVA distribution involves evaluating the expressions given in Section 1.3.2. The procedure is a bit tedious but one can go through the various cases and subcases discussed in Proposition 2.1, and compute the value of the dual minimizer α^* as given in Theorem 2.1, to recover the worst case distribution $\{(x_i^*,y_i^{c*},y_i^{f*}): i\in\{1,...,N+1\}\}$ for a given δ. This procedure is done for a few concrete examples in Section 3.

2.2.4 Discussion

One limitation in the current approach is the omission of a risk neutral measure constraint on the underlying interest rate and credit default distributions that generate the portfolio exposure distributions described by the Wasserstein ball $\mathscr{U}_{\delta_3}(\Phi_N)$. It is not clear how to (either explicitly or implicitly) incorporate such a constraint in a solvable way. We highlight this as an opportunity for improvement and a direction for further research. Empirical results for our worst case CVA studies are provided in Section 3. From the authors' perspective the computational study was illuminating to understand the magnitude and shape of worst case CVA profiles as a function of ambiguity. Some recent work was done to map Wasserstein radii into lower and upper bounds on the distance between the true and empirical distributions. See the discussion on this topic in Section 3.1.

2.3 FCA, FBA

The robust FCA can be written as

$$\sup_{P\in\mathscr{U}_{\delta_1}(P_N)}\mathbb{E}^P[\langle Z^+,Y_{CF}\rangle]P4. \tag{83}$$

Similarly, the robust FBA can be written as

$$\sup_{Q\in\mathscr{U}_{\delta_2}(Q_N)} \mathbb{E}^{Q}[\langle Z^{-}, Y_{CF}\rangle]P5. \tag{84}$$

As such, the dual formulations and solutions to the above primal optimization problems are special cases of the solutions to the FVA optimization problems, to be described next.

2.4 FVA

2.4.1 Inner Optimization Problem

The robust FVA is

$$\sup_{\Phi\in\mathscr{U}_{\delta_3}(\Phi_N)} \mathbb{E}^{\Phi}[\langle Z, Y_{CF}\rangle]P6. \tag{85}$$

Similar to before, we use recent duality results, noting the inner product $\langle\,;\rangle$ satisfies the upper semicontinuous condition of the Lagrangian duality theorem, and cost function c_S satisfies the non-negative lower semicontinuous condition (see Blanchet and Murthy (2019) Assumptions 1 & 2, Gao and Kleywegt (2016)). Hence the dual problem (to sup above) can be written as

$$\inf_{\alpha\geq 0} F(\alpha) := \left[\alpha\delta_3 + \frac{1}{N}\sum_{i=1}^{N}\Psi_\alpha(z_i, y_i^{cf})\right]D6 \tag{86}$$

where

$$\Psi_\alpha(z_i, y_i^{cf}) = \sup_{u\in\mathbb{R}^n, v\in B_n^1}[\langle u,v\rangle - \alpha c_{S_3}((u,v),(z_i,y_i^{cf}))] = \sup_{u\in\mathbb{R}^n, v\in B_n^1}[\langle u,v\rangle - \alpha(\langle u-z_i, u-z_i\rangle + S_3\langle v-y_i^{cf}, v-y_i^{cf}\rangle)]. \tag{87}$$

Now apply change of variables $w_1 = (u - z_i)$ and $w_2 = (v - y_i^{cf})$ to get

$$\Psi_\alpha(z_i, y_i^{cf}) = \sup_{w_1\in\mathbb{R}^n, w_2\in B_n^2}[\langle w_1 + z_i, w_2 + y_i^{cf}\rangle - \alpha(\langle w_1, w_1\rangle + S_3\langle w_2, w_2\rangle)] \tag{88}$$

where the sets B_n^1 and B_n^2 are defined as before. It turns out that Ψ_α can be expressed as original FVA plus the pointwise max of $(n+1)$ convex functions. The degenerate case $l = 0$ is just a line of negative slope. The other n cases are hyperbolas plus lines of negative slope. Ψ_α quantifies the adversarial move in FVA across both time and spatial dimensions while accounting for the cost via the K terms.

We have $\Psi_\alpha(z_i, y_i^{cf}) = \langle z_i, y_i^{cf}\rangle + \left[\frac{l^*}{4\alpha} + \left(\sum_{k=1}^{l^*} z_{ik} - \sum_{k=1}^{\|y_i^{cf}\|_1} z_{ik}\right) - \alpha S_3 K\right]$
where $l^* =_{l\geq 0} [\frac{l}{4\alpha} + \sum_{k=1}^{l} z_{ik} - \alpha S_3 K]$ and $l = \|w_2 + y_i^{cf}\|_1 \geq 0$, $l \in \mathbb{Z}^+$. Also $\|y_i^{cf}\|_1 \in \mathbb{Z}^+$, and $K = |l - \|y_i^{cf}\|_1| = \|w_2\|_1 \geq 0, K \in \mathbb{Z}^+$. Once l^* is selected, $K := |l^* - \|y_i^{cf}\|_1| = \|w_2^*\|_1$. Alternatively, $\Psi_\alpha(z_i, y_i^{cf}) = \langle z_i, y_i^{cf}\rangle + \bigvee_{l=0}^{n} h_\alpha(l)$ for $h_\alpha(l) := \left[\frac{l}{4\alpha} + \left(\sum_{k=1}^{l} z_{ik} - \sum_{k=1}^{\|y_i^{cf}\|_1} z_{ik}\right) - \alpha S_3 K\right]$. This result follows from jointly maximizing the adversarial funding exposure w_1 and the survival time index w_2. The structure of B_n^2 allows us to decouple this joint maximization and find the critical point to maximize the quadratic in w_1 and write down the condition to select the optimal survival time index l^*. Finally, consider the two cases $w_2 = 0$ and $w_2 \neq 0$ and take the max to arrive at the solution. The K terms represent the cost associated with the worst case.

The particular structure of B_n^1 and B_n^2 will be exploited to evaluate the sup above. The analysis proceeds by considering different cases for optimal values (w_1^*, w_2^*).

Case 1 Suppose $w_2^* = 0 l = \|y_i^{cf}\|_1$. Then

$$\Psi_\alpha(z_i, y_i^{cf}) = \langle z_i, y_i^{cf}\rangle + \sup_{w_1\in\mathbb{R}^n}[\langle w_1, y_i^{cf}\rangle - \alpha\langle w_1, w_1\rangle]. \tag{89}$$

Applying the Cauchy-Schwarz Inequality gives

$$\Psi_\alpha(z_i, y_i^{cf}) = \langle z_i, y_i^{cf}\rangle + \sup_{\|w_1\|}[\|w_1\|\|y_i^{cf}\| - \alpha\|w_1\|^2]. \tag{90}$$

Evaluating the critical point $\|w_1^*\| = \frac{\|y_i^{cf}\|}{2\alpha} \in \mathbb{R}_+$ for the quadratic gives

$$\Psi_\alpha(z_i, y_i^{cf}) = \langle z_i, y_i^{cf} \rangle + \frac{\|y_i^{cf}\|^2}{4\alpha} = \langle z_i, y_i^{cf} \rangle + \frac{\|y_i^{cf}\|_1}{4\alpha}. \tag{91}$$

Case 2 Now consider $w_2^* \neq 0 l \neq \|y_i^{cf}\|_1$.
Observe for $l = \|w_2 + y_i^{cf}\|_1 \geq 0$,

$$\langle w_1 + z_i, w_2 + y_i^{cf} \rangle = \sum_{k=1}^{l} (w_{1k} + z_{ik}). \tag{92}$$

The structure of finite set B_n^2 implies

$$\Psi_\alpha(z_i, y_i^{cf}) = \sup_{w_1 \in \mathbb{R}^n, l \in \{0,\ldots,n\}, l \neq \|y_i^{cf}\|_1} [\sum_{k=1}^{l} (w_{1k} + z_{ik}) - \alpha(\langle w_1, w_1 \rangle + S_3 K)]. \tag{93}$$

Again, using that B_n^2 is a finite set, one can write

$$\Psi_\alpha(z_i, y_i^{cf}) = \max_{l \in \{0,\ldots,n\}, l \neq \|y_i^{cf}\|_1} \sup_{w_1 \in \mathbb{R}^n} [\sum_{k=1}^{l} (w_{1k} + z_{ik}) - \alpha(\langle w_1, w_1 \rangle + S_3 K)]. \tag{94}$$

Observing that only the first l components of w_1 inside the sup are positive gives $\forall k \in \{1, \ldots, l\}$

$$\sup_{w_1 \in \mathbb{R}^n} [\sum_{k=1}^{l} (w_{1k}) - \alpha \langle w_1, w_1 \rangle] = l \times \sup_{w_{1k} \in \mathbb{R}} [w_{1k} - \alpha (w_{1k})^2]. \tag{95}$$

Evaluating at the critical point $w_{1k}^* = \frac{1}{2\alpha} \in \mathbb{R}_+$ for the above quadratic gives

$$\sup_{w_{1k} \in \mathbb{R}} [w_{1k} - \alpha (w_{1k}^2)] = \frac{1}{4\alpha}. \tag{96}$$

Therefore one can write

$$\Psi_\alpha(z_i, y_i^{cf}) = \max_{l \in \{0,\ldots,n\}, l \neq \|y_i^{cf}\|_1} [\frac{l}{4\alpha} + \sum_{k=1}^{l} (z_{ik}) - \alpha S_3 K]. \tag{97}$$

Furthermore, l^* is determined as

$$l^* = _{l \in \{0,\ldots,n\}, l \neq \|y_i^{cf}\|_1} [\frac{l}{4\alpha} + \sum_{k=1}^{l} (z_{ik}) - \alpha S_3 K]. \tag{98}$$

Substituting back into expression for Ψ_α gives

$$\Psi_\alpha(z_i, y_i^{cf}) = \langle z_i, y_i^{cf} \rangle + \left[\frac{l^*}{4\alpha} + \left(\sum_{k=1}^{l^*} z_{ik} - \sum_{k=1}^{\|y_i^{cf}\|_1} z_{ik} \right) - \alpha S_3 K \right]. \tag{99}$$

Finally, taking the max values for Ψ_α over cases $w_2^* = 0$ and $w_2^* \neq 0$ gives

$$\Psi_\alpha(z_i, y_i^{cf}) = \langle z_i, y_i^{cf} \rangle + \left[\frac{\|y_i^{cf}\|_1}{4\alpha} \right] \vee \left[\frac{l^*}{4\alpha} + \left(\sum_{k=1}^{l^*} z_{ik} - \sum_{k=1}^{\|y_i^{cf}\|_1} z_{ik} \right) - \alpha S_3 K \right]. \tag{100}$$

Observe that for $l^* = \|y_i^{cf}\|_1$, the last term in brackets $[;]$ above evaluates to $\left[\frac{\|y_i^{cf}\|_1}{4\alpha}\right]$. Let l^* be determined as

$$l^* =_{l\in\{0,\ldots,n\}} [\frac{l}{4\alpha} + \sum_{k=1}^{l}(z_{ik}) - \alpha S_3 K] \tag{101}$$

and write

$$\Psi_\alpha(z_i, y_i^{cf}) = \langle z_i, y_i^{cf}\rangle + \left[\frac{l^*}{4\alpha} + \left(\sum_{k=1}^{l^*} z_{ik} - \sum_{k=1}^{\|y_i^{cf}\|_1} z_{ik}\right) - \alpha S_3 K\right]. \tag{102}$$

Alternatively, one can write

$$\Psi_\alpha(z_i, y_i^{cf}) = \langle z_i, y_i^{cf}\rangle + \bigvee_{l=0}^{n}\left[\frac{l}{4\alpha} + \left(\sum_{k=1}^{l} z_{ik} - \sum_{k=1}^{\|y_i^{cf}\|_1} z_{ik}\right) - \alpha S_3 K\right]. \tag{103}$$

2.4.2 Outer Optimization Problem

The goal now is to evaluate

$$\inf_{\alpha\geq 0} F(\alpha) := \left[\alpha\delta_3 + \frac{1}{N}\sum_{i=1}^{N}\Psi_\alpha(z_i, y_i^{cf})\right] \tag{104}$$

where

$$\Psi_\alpha(z_i, y_i^{cf}) = \langle z_i, y_i^{cf}\rangle + \bigvee_{l=0}^{n} h_\alpha(l) \; for \; h_\alpha(l) := [\frac{l}{4\alpha} + (\sum_{k=1}^{l} z_{ik} - \sum_{k=1}^{\|y_i^{cf}\|_1} z_{ik}) - \alpha S_3 K]. \tag{105}$$

The convexity of the objective function $F(\alpha)$ simplifies the task of solving this optimization problem. The first order optimality condition suffices. As Ψ_α and hence $F(\alpha)$ may have non-differentiable kinks due to the max functions, $\vee$, we characterize the optimality condition via subgradients. In particular, we look for $\alpha^* \geq 0$ such that $0 \in \partial F(\alpha^*)$. Inspection of the asymptotic properties of Ψ_α and its subgradients reveals that $\partial F(\alpha)$ will cross zero (as α sweeps from 0 to ∞) and hence $\alpha^* \geq 0$. Note that for $\delta_3 = 0$ one recovers the expression for original FVA given in Section 1.3.5.

Let $\alpha^* \in \{\alpha \geq 0 : 0 \in \partial F(\alpha)\}$
where $\partial\Psi_\alpha = \mathbf{Conv} \cup \left\{\partial h_\alpha(l) \,|\, \langle z_i, y_i^{cf}\rangle + h_\alpha(l) = \Psi_\alpha; l \in \{0,\ldots,n\}\right\}$ and $\partial F(\alpha) = \delta_3 + \frac{1}{N}\sum_{i=1}^{N}\partial\Psi_\alpha$.

This follows from application of standard properties of subgradients as well as inspection of the asymptotic properties of Ψ_α and $\partial\Psi_\alpha$. For α sufficiently small, Ψ_α has a large positive value and $\partial\Psi_\alpha$ has a large negative derivative. For α sufficiently large, for optimal l^*, either $l^* = 00 \in \partial\Psi_\alpha$ or $l^* = \|y_i^{cf}\|_1 > 0\partial\Psi_\alpha$ approaches zero $\partial F(\alpha)$ crosses zero.

This follows from standard application of properties of convex functions and subgradients. First note that function h_α is convex in α since (for fixed l) it is the sum of a hyperbola plus a constant plus a negative linear term. So then Ψ_α is convex since it is the pointwise max of a finite set of convex functions plus a constant. Using properties of subgradients, one can write $\partial\Psi_\alpha = \mathbf{Conv} \cup \{\partial h_\alpha(l) \,|\, \langle z_i, y_i^{cf}\rangle + h_\alpha(l) = \Psi_\alpha; l \in \{0,\ldots,n\}\}$. Furthermore $F(\alpha)$ is convex in α since it is a linear term plus a sum of convex functions, so one can write $\alpha^* \in \{\alpha : 0 \in \partial F(\alpha)\}$ and it follows that $\partial F(\alpha) = \delta_3 + \frac{1}{N}\sum_{i=1}^{N}\partial\Psi_\alpha$. Finally, we argue that $\alpha^* \geq 0$. For $\alpha > 0$ sufficiently small, $\exists z < -\delta_3$ such that $z \in \partial\Psi_\alpha$ and for $\alpha > 0$ sufficiently large, $\exists z > -\delta_3$ such that $z \in \partial\Psi_\alpha$. To elaborate, for $\alpha > 0$ sufficiently large, $\|y_i^{cf}\|_1 > 0 l^* = \|y^{cf}\|_1 K = 0 \exists z > -\delta_3$ such that $z \in \partial\Psi_\alpha$. To elaborate, for $\alpha > 0$ sufficiently large, $\|y_i^{cf}\|_1 = 0 l^* = 0K = 0, \Psi_\alpha = 0, 0 = z > -\delta_3$ such that $z \in \partial\Psi_\alpha$. Hence we deduce $\partial F(\alpha)$ crosses the origin (as α sweeps from 0 to ∞).

The primal problem 85 has solution $\left[\alpha^*\delta_3 + \frac{1}{N}\sum_{i=1}^{N}\Psi_{\alpha^*}(z_i, y_i^{cf})\right]$

where $\alpha^* \in \{\alpha \geq 0 : 0 \in \partial F(\alpha)\}$ and $\Psi_{\alpha^*}(z_i, y_i^{cf}) = \langle z_i, y_i^{cf}\rangle + \bigvee_{l=0}^{n} h_{\alpha^*}(l) \; for \; h_{\alpha^*}(l) := [\frac{l}{4\alpha^*} + (\sum_{k=1}^{l} z_{ik} - \sum_{k=1}^{\|y_i^{cf}\|_1} z_{ik}) - \alpha^* S_3 K]$. Expressed in terms of original FVA, this says

$$\sup_{\Phi\in\mathscr{U}_{\delta_3}(\Phi_N)} \mathbb{E}^{\Phi}[\langle Z, Y_{CF}\rangle] = \mathbb{E}^{\Phi_N}[\langle Z, Y_{CF}\rangle] + \alpha^*\delta_3 + \mathbb{E}^{\Phi_N}[\bigvee_{l=0}^{n}\frac{l}{4\alpha^*} + (\sum_{k=1}^{l} Z_k - \sum_{k=1}^{\|Y_{CF}\|_1} Z_k) - \alpha^* S_3 K] \tag{106}$$

where the additional terms represent a penalty due to ambiguity in probability distribution. This follows directly from

the previous two propositions. $\delta_3 = 0$ reduces to original FVA. This follows by direct substitution of α^* as characterized in Proposition 2.3 into Proposition 2.2 and then the dual problem 86.

2.4.3 Recovering the Worst Case Distribution

The process of recovering the worst case FVA distribution is similar to that for CVA. In fact, for the FVA case, the procedure is a bit simpler since there are less cases and subcases to consider to recover $\{x_i^*, y_i^{cf*} : i \in \{1,...,N+1\}\}$. The steps to recover the dual minimizer α^* are the same. This procedure is done for a few concrete examples in Section 3.

2.4.4 Discussion

The comments regarding incorporation of risk neutral measure constraint for the robust CVA problem formulations apply for the robust FVA problem formulations as well. Empirical results for the worst case FVA studies are provided in Section 3. Similar to CVA, from the authors' perspective the computational study was illuminating to understand the magnitude and shape of worst case FVA profiles as a function of ambiguity.

3. Computational Study: Robust XVA and Wrong Way Risk

This computational study uses the Matlab Financial Instruments Toolbox and extends WWR portfolio analysis (Brigo et al., 2013, section 5.3) to consider ambiguity in probability distribution. Other key concepts that will be discussed in this section include suitable choice for Wasserstein radius δ, calibration of scale factor S_3, and choice of units for exposures. The studies in this section will investigate (and quantify) worst case bilateral CVA and FVA for different market environments and portfolios of interest rate swaps. For CVA, the current swaps market data (see below) will be used in conjunction with monte carlo simulation of a market calibrated one factor Hull-White model for interest rates. The counterparty credit curve selection will vary between investment grade and high yield. For FVA, the funding spreads and volatility data is taken from Markit. The swaps portfolios are shown as well. All calculations are done in Matlab using the financial instruments toolbox (Matlab, 2019).

3.1 Suitable Choice for Wasserstein Radius

A natural question to ask when computing worst case XVA is how to interpret the size of the Wasserstein radius δ. A discussion of some key results is given in (Carlsson et al., 2018, Section 3). For this study, we adopt a fairly straightforward approach to compute upper and lower bounds for the expected Wasserstein distance between the empirical and true distributions. A rough procedure for selecting δ involves sampling two independent data sets D_1 *and* D_2, and setting $\delta = \alpha c^*$ where $\alpha \in [1/2, 1]$ and c^* denotes the cost of the minimum bipartite matching between D_1 *and* D_2 (Carlsson et al., 2018), (Canas and Rosasco, 2012). This approach relies on the following theorem referenced in Carlsson et al. (2018) and established in Canas and Rosasco (2012). Let $\hat{f}_1$ and $\hat{f}_2$ denote empirical distributions associated with two sets of independent samples of n points from a distribution f. Then

$$\frac{1}{2}\mathbb{E}\left[D_c(\hat{f}_1, \hat{f}_2)\right] \leq \mathbb{E}\left[D_c(f, \hat{f}_1)\right] \leq \mathbb{E}\left[D_c(\hat{f}_1, \hat{f}_2)\right].$$

As such, our approach is to sample two indepedent data sets D_1 and D_2 of portfolio exposures and default times and compute lower and upper bounds $\delta^l := \frac{1}{2}\mathbb{E}\left[D_c(\hat{f}_1, \hat{f}_2)\right]$ and $\delta^u := \mathbb{E}\left[D_c(\hat{f}_1, \hat{f}_2)\right]$ for the expected Wasserstein distance between the empirical and true distributions. Given these bounds, one can compute the corresponding lower and upper bounds on the worst case XVA risk metrics and exposure and default time distributions.

Constructing the bounds δ^l and δ^u in this way builds in a dependency on the units of portfolio exposures (e.g. millions of dollars) and units in the time dimension (e.g. years), through the computation of $D_c(\hat{f}_1, \hat{f}_2)$ and the calibration of the scale factor S_3 (see Section 3.2 below for this). Such a dependency is desirable to assign "units" to δ as well as to conduct relative value analysis across portfolios. See Section 3.3 below for more commentary on choice of units for exposures.

3.2 Calibration of Scale Factors

3.2.1 Calibration of S_3 for CVA

The scale factor S_3 represents a scaling for changes to default times. A suitable choice for S_3 is one that charges an appropriate cost for this. Let us think about what a change in default time means in the context of CVA. For a fixed path with index i, and exposure vector $x_i^{\pm}$, changing the default time from τ_2 to τ_1 changes the value of the realized exposure from $x_{i\tau_2}^{\pm}$ to $x_{i\tau_1}^{\pm}$ upon default. A reasonable value for S_3, call it s_3, for this particular path, might be $\|x_{i\tau_1}^{\pm} - x_{i\tau_2}^{\pm}\|_\infty$ where $\tau_1, \tau_2 \in \{1,...,n\}$. Now let us generalize this to average over all paths $i \in \{1,...,N\}$ in our empirical distribution Φ_N. Let $\overline{x_\tau^{\pm}}$ denote $\frac{1}{N}\sum_{i=1}^N x_{i\tau}^{\pm}$, the average exposure at default time τ. Substituting average exposures into our previous expression gives the relation $S_3 := \|\overline{x_{\tau_1}^{\pm}} - \overline{x_{\tau_2}^{\pm}}\|_\infty$. Let us use this as our working definition for S_3 for unilateral CVA, DVA. Calibration is straightforward given Φ_N, the set of sample paths $\{(x_i, y_i^c, y_i^f) : i \in \{1,...,N\}\}$. For bilateral CVA, take the average over

the unilateral CVA and DVA scale factors, namely $S_3 := \frac{1}{2}(\|\overline{x^+_{\tau_1}} - \overline{x^+_{\tau_2}}\|_\infty + \|\overline{x^-_{\tau_1}} - \overline{x^-_{\tau_2}}\|_\infty)$.

3.2.2 Calibration of S_3 for FVA

Let us the follow the approach above for FVA. For a fixed path with index i, the funding exposure vector is $z^\pm_i$ and the incremental change is $\Delta z^\pm_{i\tau_2}$. A reasonable value for S_3, call it s_3, for this particular path, might be $\|z^\pm_{i\tau_1} - z^\pm_{i\tau_2}\|_\infty$. Substituting average exposures into this expression gives the relation $S_3 := \|\overline{z^\pm_{\tau_1}} - \overline{z^\pm_{\tau_2}}\|_\infty$. Let us use this as our working definition for S_3 for FCA, FBA. Calibration is straightforward given Φ_N, the set of sample paths $\{(z_i, y^{cf}_i) : i \in \{1,...,N\}\}$. For FVA, take the average over the FCA and FBA scale factors, namely $S_3 := \frac{1}{2}(\|\overline{z^+_{\tau_1}} - \overline{z^+_{\tau_2}}\|_\infty + \|\overline{z^-_{\tau_1}} - \overline{z^-_{\tau_2}}\|_\infty)$.

3.3 Choice of Units for Exposures

Standardizing the units across portfolios is useful for relative value analysis. The choice of units for exposures (e.g. millions of dollars) and default times (e.g. decimal years) is up to the user, although we recommend these conventions, and use them in our analysis in this section. Note that different choices of units will lead to calibrated different values for S_3 for BCVA and FVA. There is no *one* choice for units (as in regression analysis, for example) although consistency is recommended as a good practice. The same comments apply for the choices of time frequency and time horizon for the robust XVA analysis.

3.4 Definitions for Exposure Calculations

The definitions for the various exposure calculations plotted in Section 3.6 for CVA and DVA are given in Table 2 below. For FVA calculations (FCA and FBA), plotted in Section 3.7, replace portfolio exposures V^+ and V^- with funding exposures Z^+ and Z^- respectively.

Table 2. CVA Exposure Calculations

Term	CVA^U	DVA^U
$EE(t)$	$\mathbb{E}[V^+(t)]$	$\mathbb{E}[V^-(t)]$
$PFE_\alpha(t)$	$\inf\{x \in \mathbb{R} : \alpha \le F_{V^+(t)}(x)\}$	$\inf\{x \in \mathbb{R} : \alpha \le F_{V^-(t)}(x)\}$
$EPE(t)$	$\frac{1}{T}\int_0^T EE(t)dt$	$\frac{1}{T}\int_0^T EE(t)dt$
$EffEE(t)$	$\max\{EE(\tau) : \tau \in [0,t]\}$	$\max\{EE(\tau) : \tau \in [0,t]\}$
$EffEPE(t)$	$\frac{1}{T}\int_0^T EffEE(t)dt$	$\frac{1}{T}\int_0^T EffEE(t)dt$

standard definitions

3.5 Market Data

As of April 20, 2020, the 5y par interest rate swap rate is 0.47% (on Bloomberg). The full interest rate swaps curve is shown in Table 3. All market data displayed below is for this date.

Table 3. Swap Rates

Swap Tenor	1y	2y	3y	5y	7y	10y	30y
Swap Rate	0.515%	0.409%	0.401%	0.470%	0.569%	0.691%	0.855%

term structure of par coupon fixed floating swap rates

Bloomberg shows the interest rate swaption volatility matrix (with option expirations as rows and swap tenors as columns).

Table 4. Swaption Normal Volatilities

Exp / Tenor	2y	3y	5y	7y	10y
2y	0.520%	0.542%	0.601%	0.631%	0.680%
3y	0.577%	0.592%	0.622%	0.640%	0.671%
5y	0.637%	0.637%	0.637%	0.643%	0.652%
7y	0.640%	0.639%	0.636%	0.636%	0.636%
10y	0.639%	0.633%	0.624%	0.618%	0.612%

term structure of at-the-money swaption volatilities

Furthermore, Markit shows U.S. CDX investment grade and high yield 5y credit default swap spreads as in Table 5. The firm and counterparty investment grade credit spreads are set to 100 and 150 basis points respectively. The high yield credit spreads are shown in Table 6. Referencing MarkIt funding spreads, the funding spread curves are shown in Table 7. Unavailable quotes for high yield spreads are displayed as "N/A". This term structure of funding spreads is used for the FVA analysis. Funding spread lognormal volatility is set to exponential decay. For investment grade it decays from 85% down to about 31% in 10 years. For high yield it decays from 35% down to about 13%.

Table 5. 5y CDS Spreads

CDX Index	IG	HY
CDS Spread	0.933%	6.432%

credit default swap spreads

Table 6. High Yield Counterparty Credit Spreads

CDS Tenor	1y	2y	3y	4y	5y	6y	7y	8y	9y	10y
HY Spread	6.00%	5.75%	5.50%	5.25%	5.00%	4.75%	4.50%	4.25%	4.00%	3.75%

term structure of credit default swap spreads

Talbe 7. Funding Spreads

Funding Tenor	1y	2y	3y	5y	7y	10y
IG Spread	0.54%	0.81%	0.81%	0.88%	1.01%	1.14%
HY Spread	N/A	N/A	8.02%	6.72%	7.08%	6.36%

term structure of funding spreads

The swaps portfolios for the CVA and FVA studies are shown in Tables 8 and 9. All 10 swaps are used for the 30y monte carlo simulation for CVA. The last 4 are capped at 10y maturity for FVA, as we have (only) 10y of funding market data.

Table 8. CVA Swaps Portfolio

Issued	Notional	Maturity	Rec / Pay Fixed	Coupon	Freq
4/20/20	10	4/20/21	Rec	0.51%	quarterly
4/20/20	10	4/20/22	Pay	0.41%	quarterly
4/20/20	10	4/20/23	Pay	0.40%	quarterly
4/20/20	10	4/20/25	Rec	0.47%	quarterly
4/20/20	10	4/20/27	Pay	0.57%	quarterly
4/20/20	10	4/20/30	Rec	0.69%	quarterly
4/20/20	10	4/20/35	Rec	0.74%	quarterly
4/20/20	10	4/20/40	Rec	0.83%	quarterly
4/20/20	10	4/20/45	Pay	0.83%	quarterly
4/20/20	10	4/20/50	Pay	0.85%	quarterly

individual swap positions in the portfolio

Table 9. FVA Swaps Portfolio

Issued	Notional	Maturity	Rec / Pay Fixed	Coupon	Freq
4/20/20	100	4/20/21	Pay	0.51%	quarterly
4/20/20	100	4/20/22	Rec	0.41%	quarterly
4/20/20	100	4/20/23	Rec	0.40%	quarterly
4/20/20	100	4/20/25	Pay	0.47%	quarterly
4/20/20	100	4/20/27	Rec	0.57%	quarterly
4/20/20	100	4/20/30	Pay	0.69%	quarterly
4/20/20	100	4/20/30	Pay	0.74%	quarterly
4/20/20	100	4/20/30	Pay	0.83%	quarterly
4/20/20	100	4/20/30	Rec	0.83%	quarterly
4/20/20	100	4/20/30	Rec	0.85%	quarterly

individual swap positions in the portfolio

3.6 Bilateral CVA

3.6.1 Investment Grade Counterparty and Firm

The swaps portfolio shown in Table 8 is used for this analysis. The portfolio consists of ten par coupon interest rate swaps, with a mix of receving fixed and paying fixed swaps at different maturities. The investment grade firm and counterparty credit spreads are set to 100 and 150 basis points respectively. The calibrated value of S_3 is 1.4584 which results in $\delta^l = 14.414$ and $\delta^u = 28.828$ using a second set of Bloomberg market data (for 03/20/20) along with the first set for 04/20/20. The full range of Wasserstein radii δ is given in Table 10.

Table 10. BCVA Wasserstein Radii

Percentage of δ^u	50%	60%	70%	80%	90%	100%
W Radius delta	14.41	17.30	20.18	23.06	25.95	28.83

range of δ that covers the true distribution f

Matlab plots characterizing the BCVA positive and negative exposure profiles and trajectory of worst case BCVA as a function of Wasserstein radius are shown in Figures 1,2,3.

The baseline BCVA for this portfolio is approximately 160k USD and represents the dot product of the discounted positive portfolio exposure profile times counterparty default probability plus dot product of the discounted negative portfolio exposure times firm default probability. The worst case BCVA curve is shown in Figure 3. The worst case CVA curve ranges from 69% to 93% the size of Max PFE (Potential Future Exposure) which is equal to 6.43mm USD (see Figure 1), for Wasserstein radii δ given in Table 10. So the takeaway here is worst case BCVA can be a significant percentage of PFE for swap portfolios with low risk counterparty default curves (investment grade).

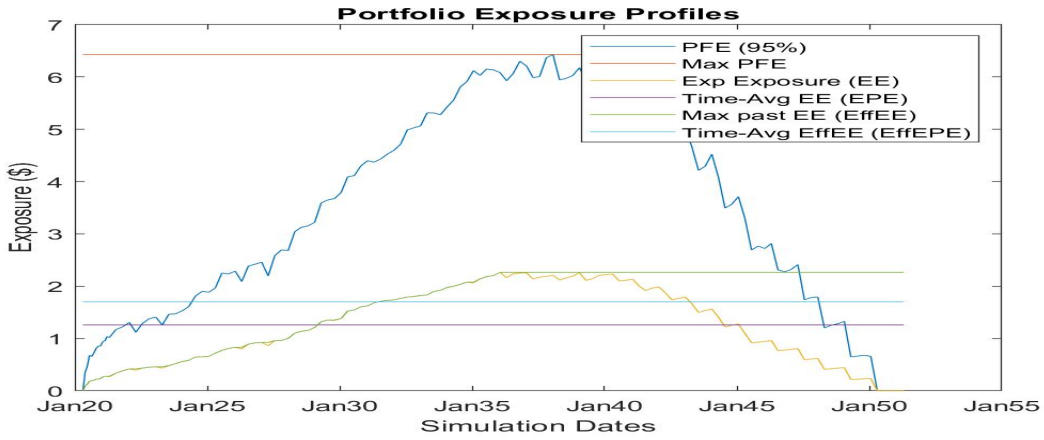

Figure 1. Swaps Portfolio Positive Exposure Profiles

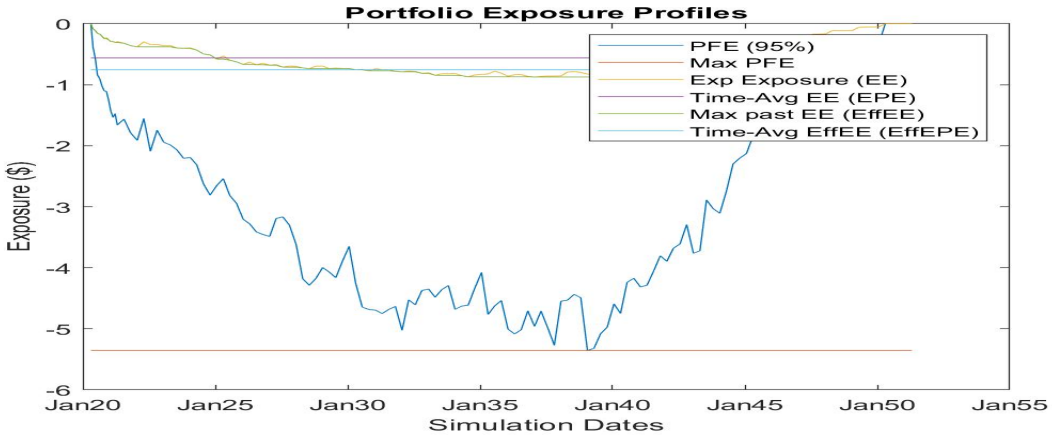

Figure 2. Swaps Portfolio Negative Exposure Profiles

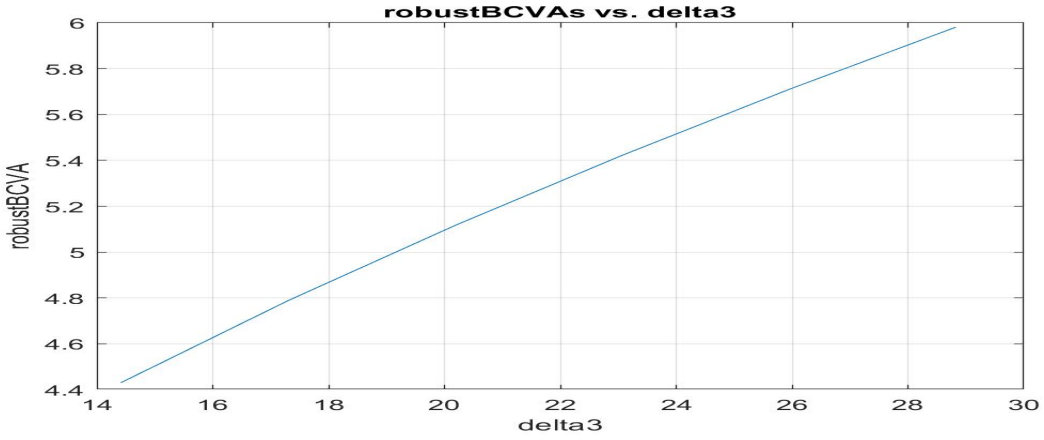

Figure 3. Swaps Portfolio Worst Case BCVA Profile

The worst case distribution for δ^u is shown in Figures 4 and 5. The first plot shows the exposures $\{x_i^*\}$ and the second plot shows the joint distribution of counterparty and firm default times $\{y_i^{c*}, y_i^{f*}\}$. Default times beyond the portfolio maturity date denote no default prior to portfolio maturity for those simulation paths. This results in higher contours in the back row.

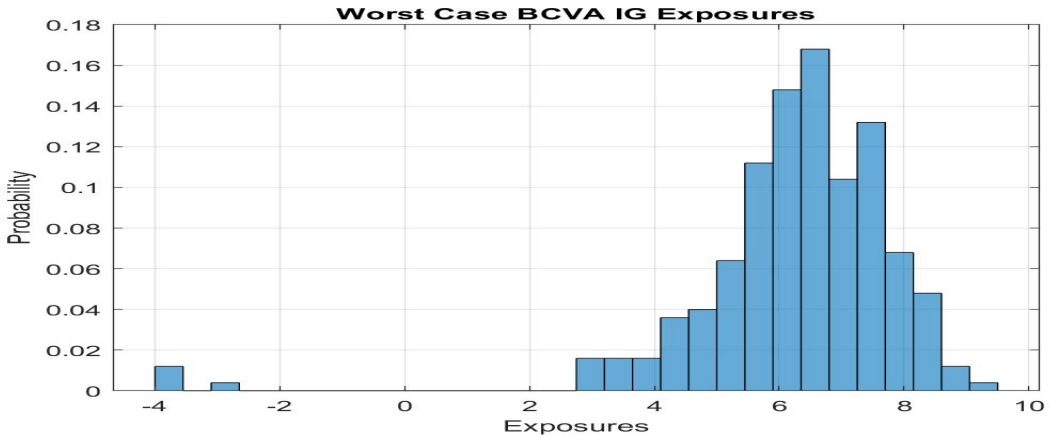

Figure 4. Worst Case Exposures

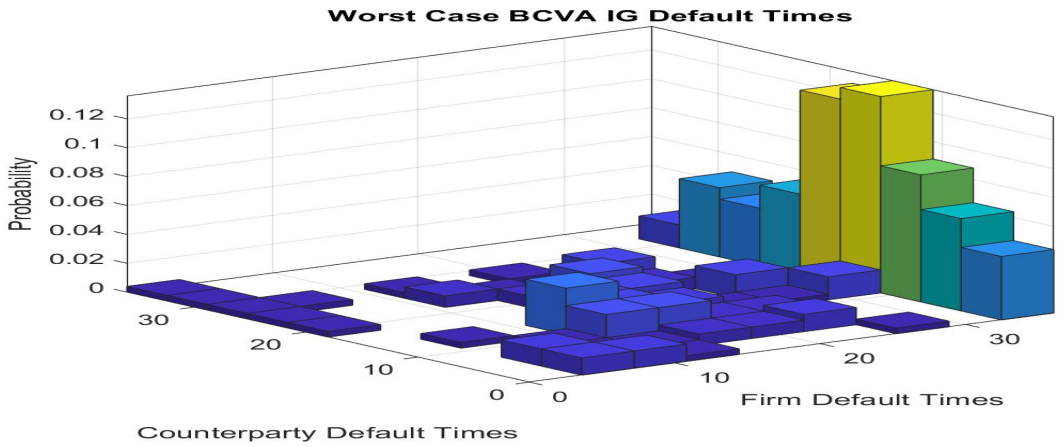

Figure 5. Worst Case Default Times

3.6.2 High Yield Counterparty and Investment Grade Firm

The swaps portfolio shown in Table 8 is used for this analysis. The portfolio consists of ten par coupon interest rate swaps, with a mix of receving fixed and paying fixed swaps at different maturities. The high yield counterparty credit spreads are set as in Table 6. The investment grade firm credit spreads are set to a constant 100 basis points. The calibrated value of S_3 is 1.4584 which results in $\delta^l = 14.45$ and $\delta^u = 28.90$ using a second set of Bloomberg market data (for 03/20/20) along with the first set for 04/20/20. The full range of Wasserstein radii δ is given in Table 11. Matlab plots characterizing the BCVA positive and negative exposure profiles and trajectory of worst case BCVA as a function of Wasserstein radius are shown in Figures 6,7,8.

Table 11. BCVA Wasserstein Radii

Percentage of δ^u	50%	60%	70%	80%	90%	100%
W Radius delta	14.45	17.34	20.23	23.12	26.01	28.90

range of δ that covers the true distribution f

The baseline BCVA for this portfolio is approximately 106k USD and represents the dot product of the discounted positive portfolio exposure profile times counterparty default probability plus dot product of the discounted negative portfolio exposure times firm default probability. The worst case BCVA curve is shown in Figure 8. Note that for this problem instance, the worst case BCVA results for high yield counterparty credit are similar to the previous subsection, for investment grade counterparty credit. Note the worst case BCVA ranges from 70% to 95% the size of Max PFE (Potential

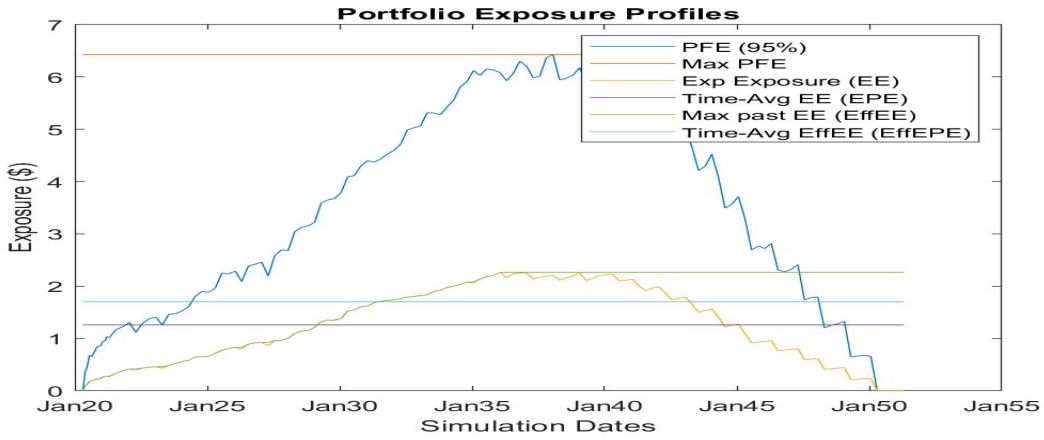

Figure 6. Swaps Portfolio Positive Exposure Profiles

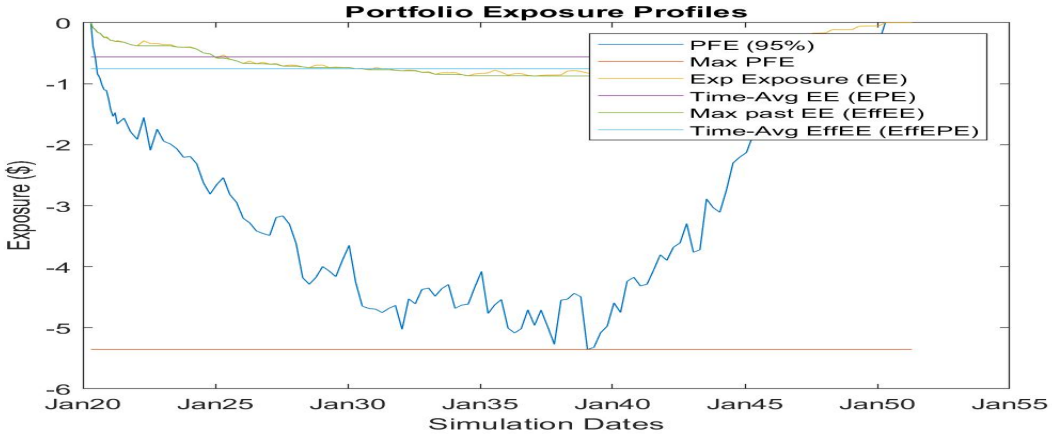

Figure 7. Swaps Portfolio Negative Exposure Profiles

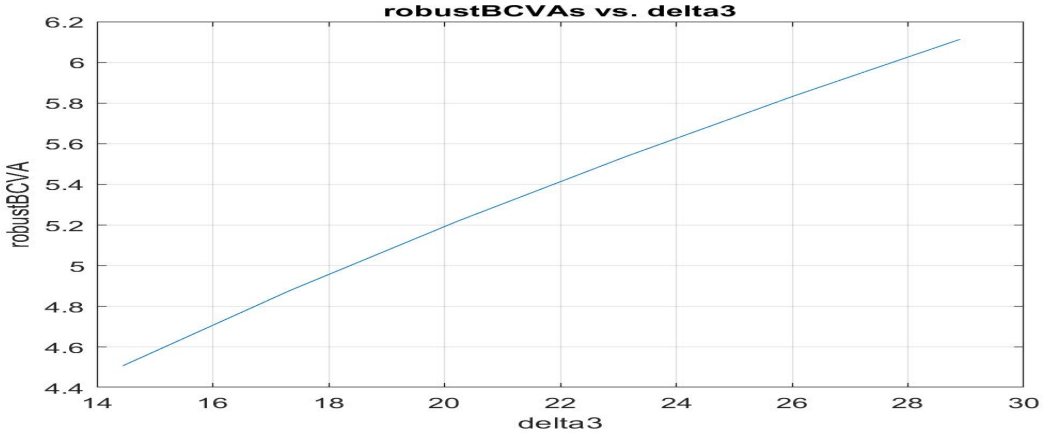

Figure 8. Swaps Portfolio Worst Case BCVA Profile

Future Exposure), which is equal to 6.43mm USD (see Figure 6), for Wasserstein radii δ given in Table 11. So the take-away here is worst case BCVA can be a significant percentage of PFE for swap portfolios with high yield counterparty default curves as well.

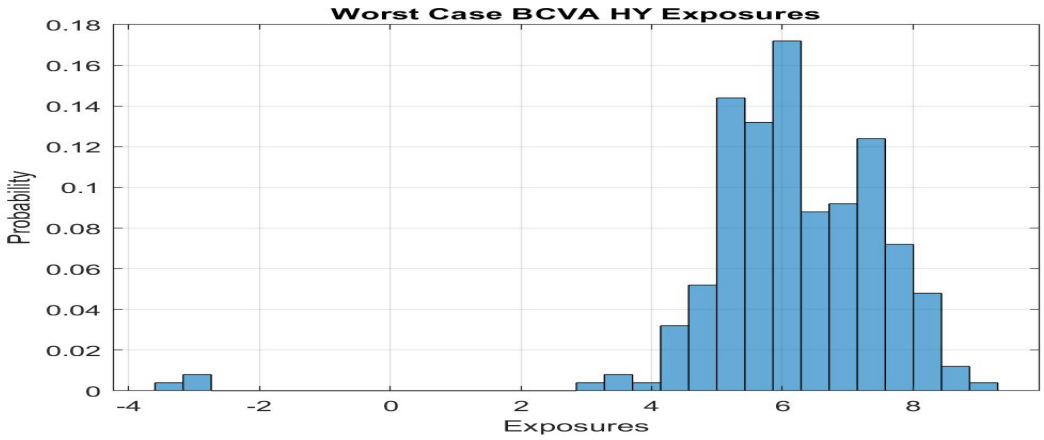

Figure 9. Worst Case Exposures

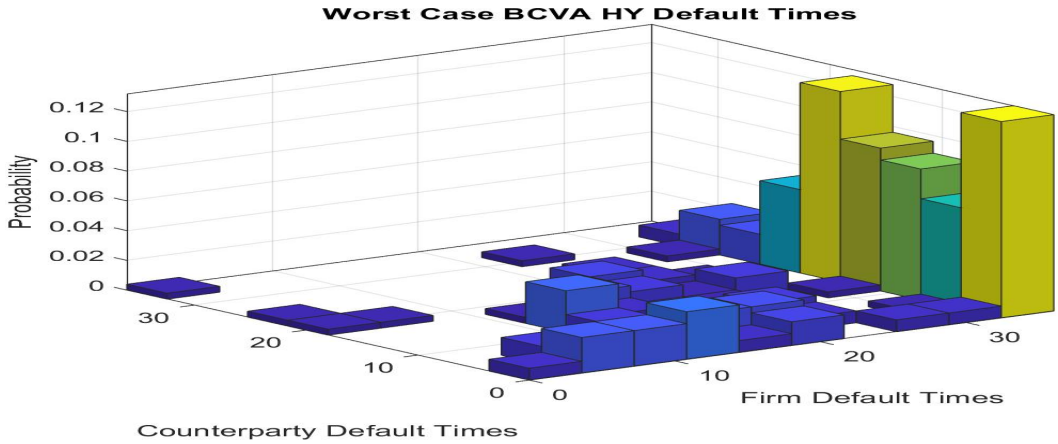

Figure 10. Worst Case Default Times

The worst case distribution for delta value δ^u is shown in Figures 9 and 10. The first plot shows the exposures $\{x_i^*\}$ and the second plot shows the joint distribution of counterparty and firm default times $\{y_i^{c*}, y_i^{f*}\}$. Default times beyond the portfolio maturity date denote no default prior to portfolio maturity for those simulation paths. This results in higher contours in the joint density plot in the back row. Higher counterparty credit spreads lead to earlier counterparty default times.

3.7 FVA

3.7.1 Investment Grade Counterparty and Firm

The swaps portfolio shown in Table 9 is used for this analysis. The portfolio consists of ten interest rate swaps, with a mix of receving fixed and paying fixed swaps at different maturities. Capping maturities at 10y introduces some positive NPV to this portfolio. The investment grade firm and counterparty funding spreads are set as shown in Table 7. The calibrated value of S_3 is 0.082 which results in $\delta^l = 0.387$ and $\delta^u = 0.774$ using a second set of Bloomberg market data (for 03/20/20) along with the first set for 04/20/20. The full range of Wasserstein radii δ is given in Table 12. Matlab plots characterizing the FVA positive and negative exposure profiles and trajectory of worst case FVA as a function of Wasserstein radius are shown in Figures 13,14,15.

Table 12. FVA Wasserstein Radii

Percentage of δ^u	0.50	0.60	0.70	0.80	0.90	1.0
W Radius delta	0.387	0.464	0.542	0.560	0.697	0.774

range of δ that covers the true distribution f

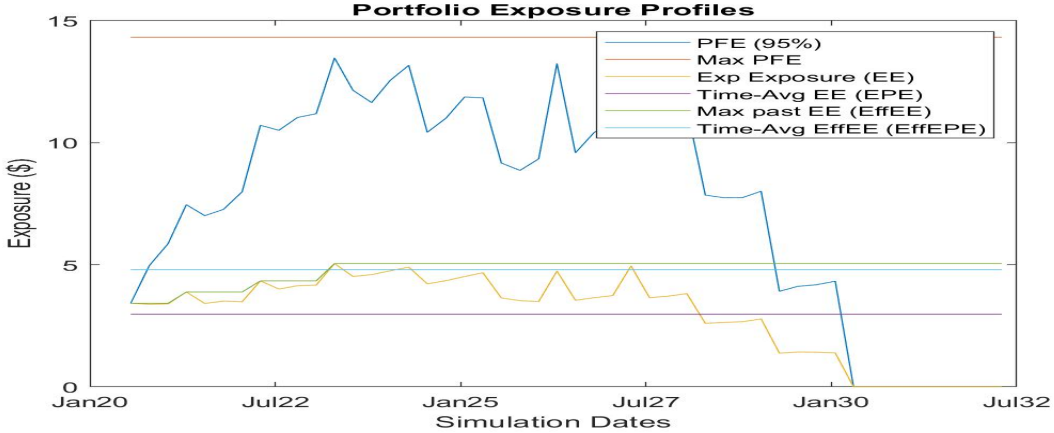

Figure 11. Swaps Portfolio Positive Exposure Profiles

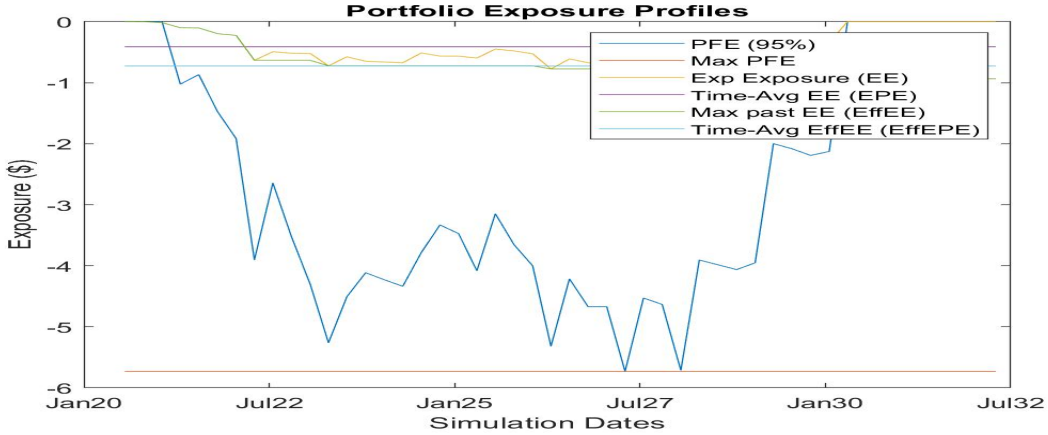

Figure 12. Swaps Portfolio Negative Exposure Profiles

The baseline FVA for this portfolio is 240k USD and represents the dot product of the discounted portfolio FCA exposure profile times joint survival probability plus dot product of the discounted portfolio FBA exposure times joint survival probability. The worst case FVA curve is shown in Figure 15. For Wasserstein radius $\delta^l = 0.387$, the worst case FVA is approximately 4.55, or 3.0 times the size of integrated FCA PFE which is about 1.54. For Wasserstein radius $\delta^u = 0.774$, the worst case FVA is approximately 5.72, or 3.7 times the size of integrated FCA PFE. In this problem instance, worst case FVA is a multiple of integrated FCA PFE exposure, so quite significant.

The worst case distribution for delta value δ^u is shown in Figures 16 and 17. The first plot shows the exposures $\{z_i^*\}$ and the second plot shows the joint distribution of counterparty and firm survival times $\{y_i^{cf*}\}$. Survival times beyond the portfolio maturity date denote no defaults prior to portfolio maturity for those simulation paths.

3.7.2 High Yield Counterparty and Investment Grade Firm

The swaps portfolio is shown in Table 8. The firm and counterparty funding spreads are set as in Table 7. The high yield counterparty credit spreads are set as shown in Table 5. The investment grade firm credit spreads are set to a constant 100 basis points. The calibrated value of S_3 is 0.2898 which results in $\delta^l = 1.935$ and $\delta^u = 3.87$ using a second set of

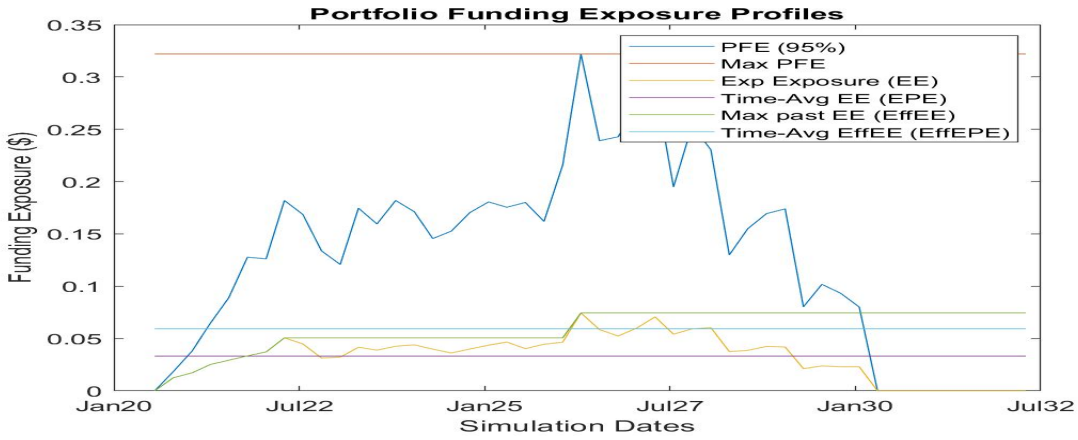

Figure 13. Swaps Portfolio IG FCA Exposure Profiles

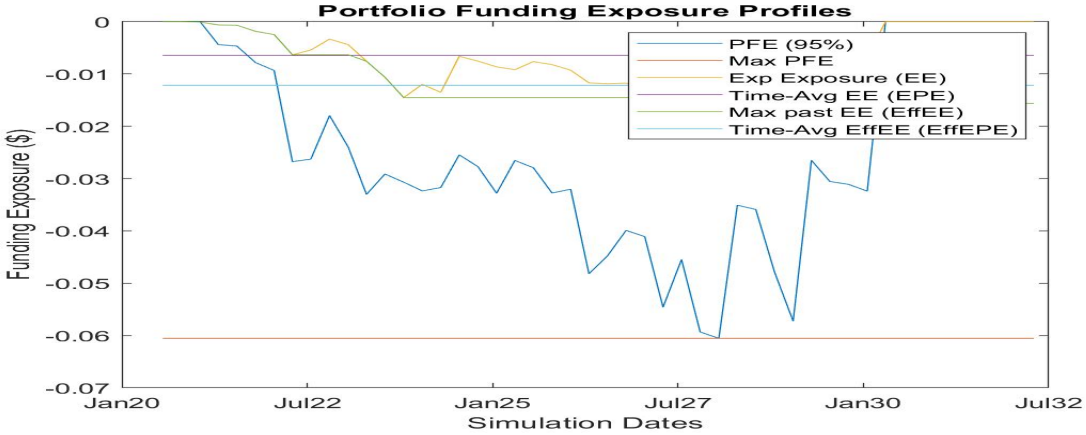

Figure 14. Swaps Portfolio IG FBA Exposure Profiles

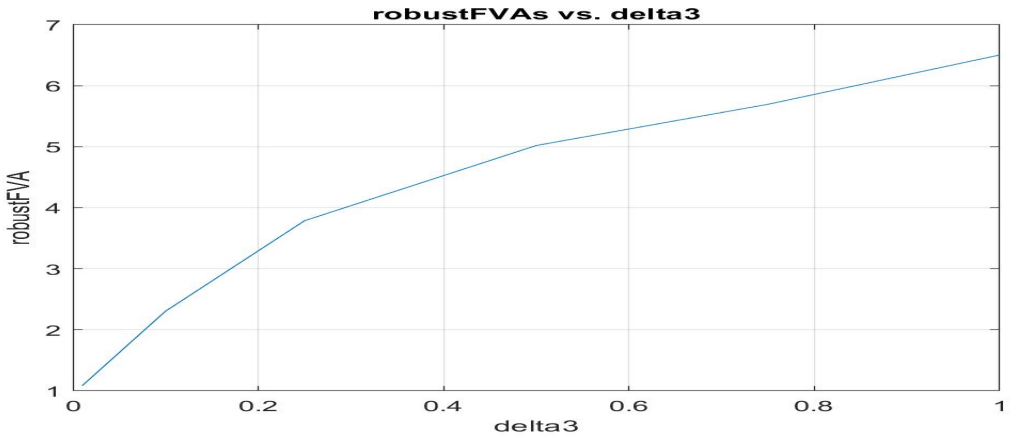

Figure 15. Swaps Portfolio Worst Case IG FVA Profile

Bloomberg market data (for 03/20/20) along with the first set for 04/20/20. The full range of Wasserstein radii δ is given in Table 13. Matlab plots characterizing the FVA positive and negative exposure profiles and trajectory of worst case FVA as a function of Wasserstein radius are shown in Figures 20,21,22.

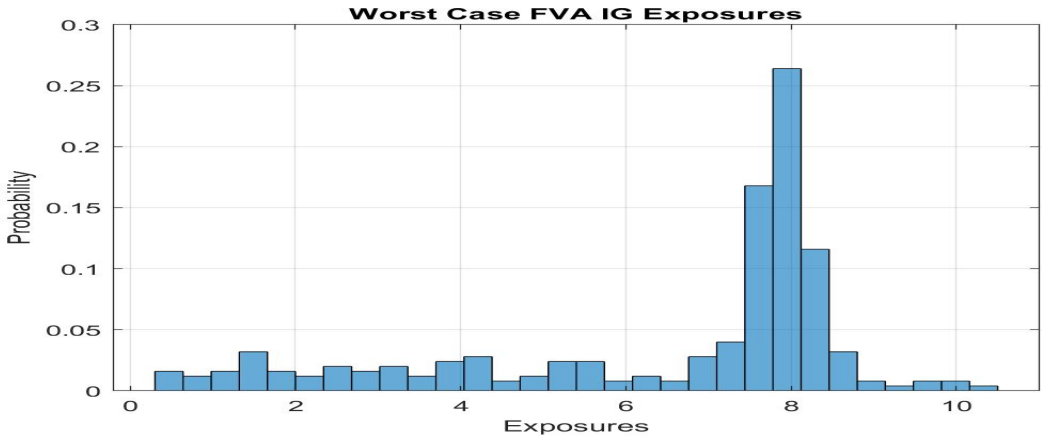

Figure 16. Worst Case Exposures

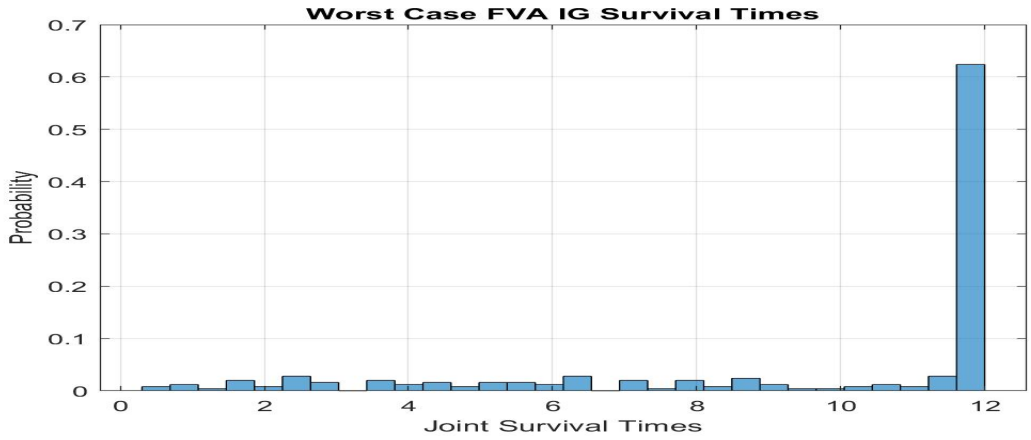

Figure 17. Worst Case Survival Times

Table 13. FVA Wasserstein Radii

Percentage of δ^u	0.50	0.60	0.70	0.80	0.90	1.0
W Radius delta	1.935	2.322	2.709	3.096	3.483	3.87

range of δ that covers the true distribution f

The baseline FVA for this portfolio is 1.18mm USD. The worst case FVA curve is shown in Figure 22. For Wasserstein radius $\delta^l = 1.935$, the worst case FVA is approximately 9.35, or 1.31 times the size of integrated FCA PFE which is about 7.127. For Wasserstein radius $\delta^u = 3.87$, the worst case FVA is approximately 12.44, or 1.75 times the size of integrated FCA PFE. In this problem instance, similar to the investment grade example, worst case FVA is a multiple of integrated FCA PFE exposure, so quite significant.

The worst case distribution for delta value δ^u is shown in Figures 23 and 24. The first plot shows the exposures $\{z_i^*\}$ and the second plot shows the joint distribution of counterparty and firm survival times $\{y_i^{cf*}\}$. Survival times beyond the portfolio maturity date denote no defaults prior to portfolio maturity for those simulation paths.

4. Conclusions and Further Work

This work has developed theoretical results and investigated calculations of robust CVA, FVA, and wrong way risk for OTC derivatives under distributional uncerainty using Wasserstein distance as an ambiguity measure. The financial market overview, foundational notation, and robust XVA primal problems were introduced in Section 1. Using recent duality results (Blanchet and Murthy, 2019), the simpler dual formulations and their analytic solutions for BCVA and FVA were

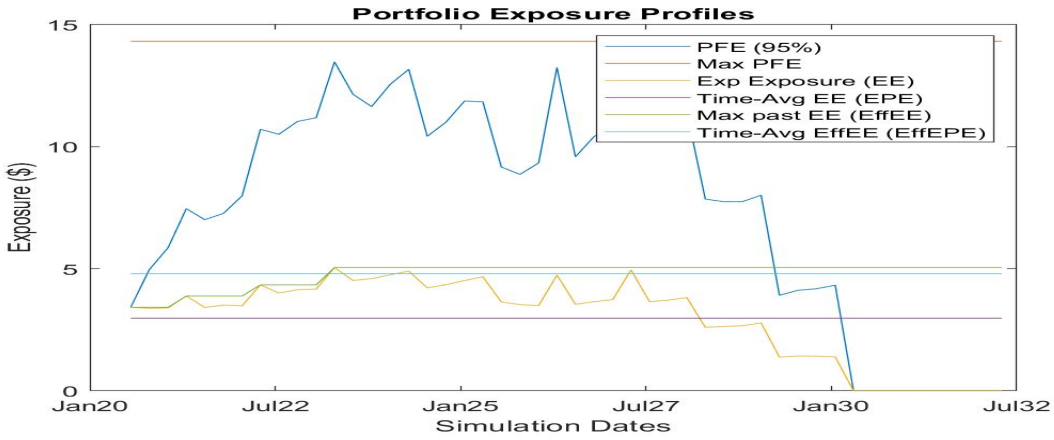

Figure 18. Swaps Portfolio Positive Exposure Profiles

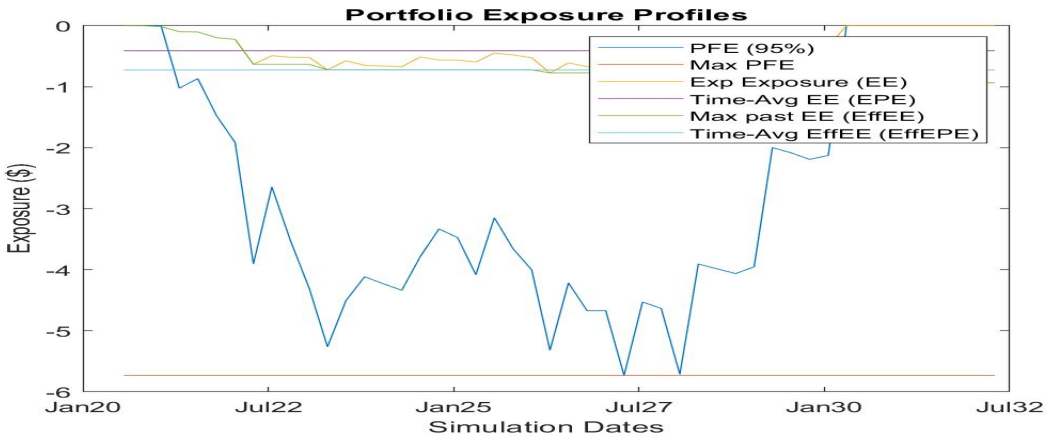

Figure 19. Swaps Portfolio Negative Exposure Profiles

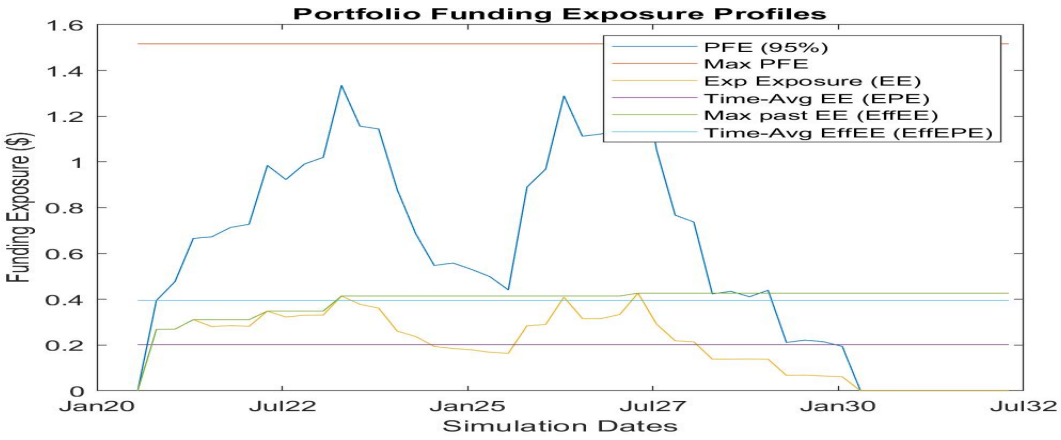

Figure 20. Swaps Portfolio HY FCA Exposure Profiles

derived in Section 2. After that, in Section 3, some computational experiments were conducted to measure the additional XVA charge due to distributional ambiguity for a variety of portfolio and market configurations. Worst case BCVA and FVA were found to be significant relative to their respective PFE profiles in all problem instances. Finally, we conclude with some commentary on directions for further research.

One direction for future research, as has been previously discussed, is to extend the problem formulations to include

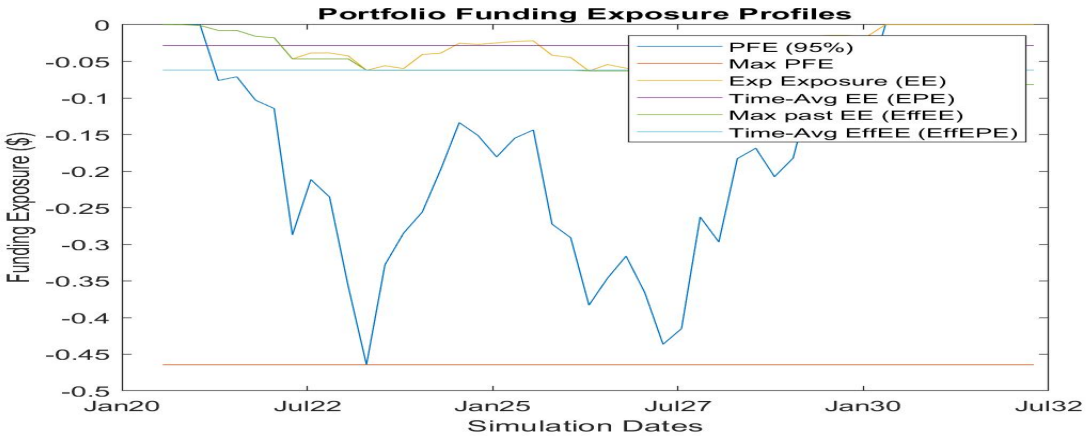

Figure 21. Swaps Portfolio HY FBA Exposure Profiles

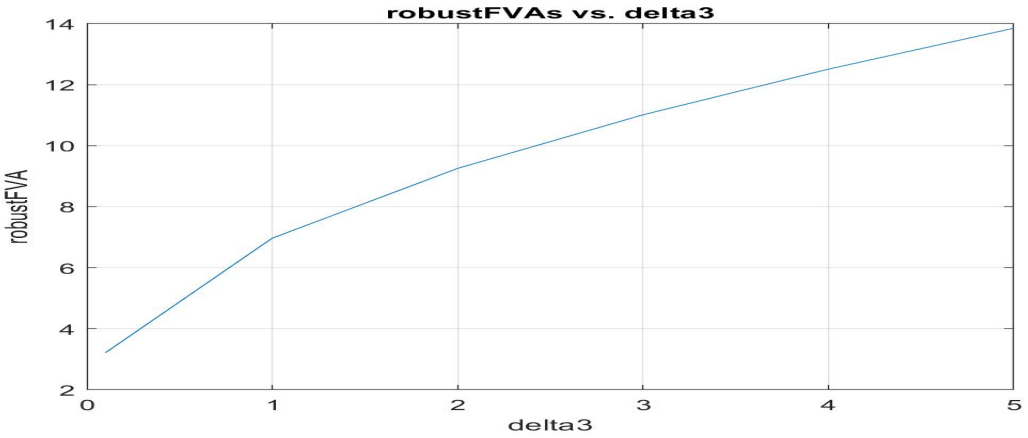

Figure 22. Swaps Portfolio Worst Case HY FVA Profile

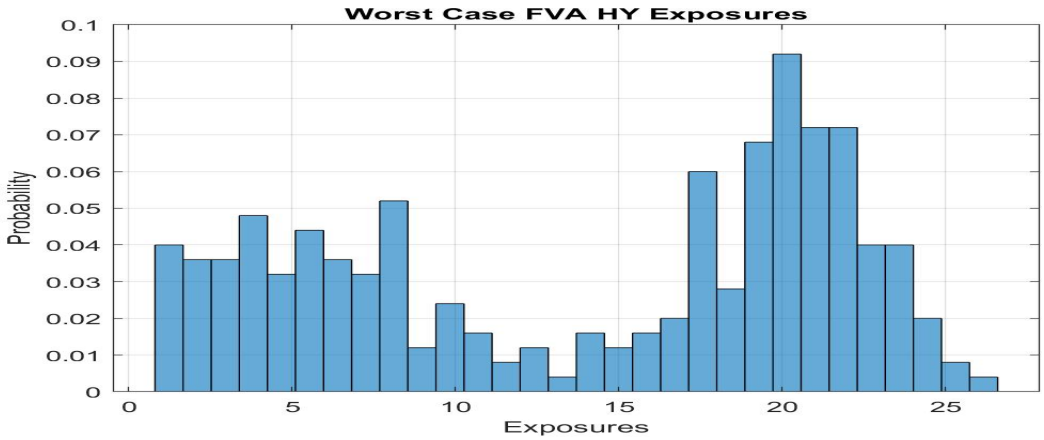

Figure 23. Worst Case Exposures

a risk neutral measure constraint in a solvable way. Explicitly adding the constraint would complicate the problem formulations no doubt, so perhaps there is a more tractable indirect approach. Another direction for future research would be to develop (and apply) similar theoretical machinery as used for robust CVA and FVA towards robust KVA (Capital Valuation Adjustment) and MVA (Margin Valuation Adjustment) and wrong way risk in that context. Intuitively, wrong way risk arises in that context when the market cost of capital and/or funding the margin position increases at the same

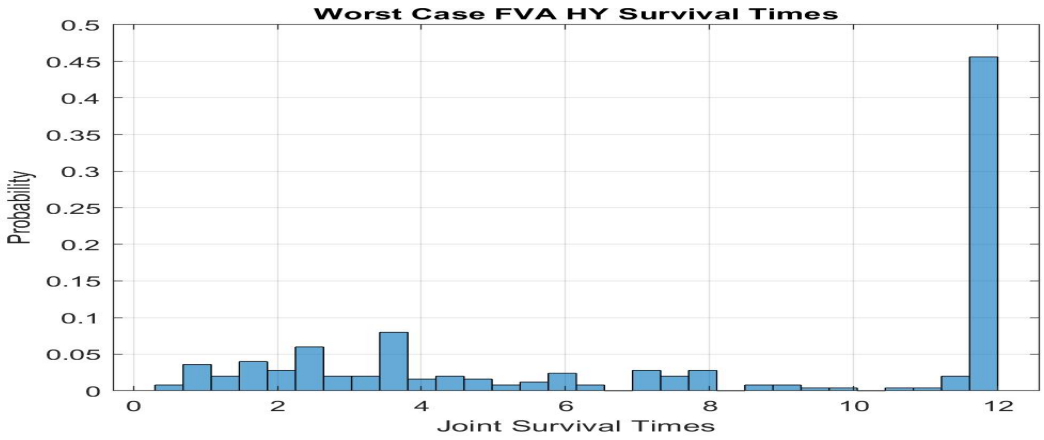

Figure 24. Worst Case Survival Times

time as the portfolio exposure increases.

Data and Code Availability Statement

The raw and/or processed data and Matlab code required to reproduce the findings from this research can be obtained from the corresponding author, [D.S.], upon reasonable request.

Conflict of Interest Statement

The authors declare they have no conflict of interest.

Funding Statement

The authors received no specific funding for this work.

References

Bartl, D., Drapeau, S., & Tangpi, L. (2017). *Computational aspects of robust optimized certainty equivalents and option pricing.*

Basel Committee on Banking Supervision. (2015). *Review of the credit valuation adjustment risk framework.*

Blanchet, J., Chen, L., & Zhou, X. Y. (2018). *Distributionally robust mean-variance portfolio selection with wasserstein distances.*

Blanchet, J., Kang, Y., & Murthy, K. (2016a). *Robust wasserstein profile inference and applications to machine learning. arXiv preprint arXiv:1610.05627.*

Blanchet, J., Kang, Y., & Murthy, K. (2016b). *Robust wasserstein profile inference and applications to machine learning. arXiv preprint arXiv:1610.05627.*

Blanchet, J., & Murthy, K. (2019). Quantifying distributional model risk via optimal transport. *Mathematics of Operations Research*, *44*(2), 565-600.

Brigo, D., Morini, M., & Pallavicini, A. (2013). *Counterparty credit risk, collateral and funding: with pricing cases for all asset classes*, volume 478. John Wiley & Sons.

Canas, G., & Rosasco, L. (2012). Learning probability measures with respect to optimal transport metrics. In *Advances in Neural Information Processing Systems*, pp. 2492-2500.

Carlsson, J. G., Behroozi, M., & Mihic, K. (2018). Wasserstein distance and the distributionally robust tsp. *Operations Research*, *66*(6), 1603-1624.

El Hajjaji, O., & Subbotin, A. (2015). Cva with wrong way risk: Sensitivities, volatility and hedging. *International Journal of Theoretical and Applied Finance*, 18(03), 1550017.

Esfahani, P. M., & Kuhn, D. (2018). Data-driven distributionally robust optimization using the wasserstein metric: Performance guarantees and tractable reformulations. *Mathematical Programming*, *171*(1-2), 115-166.

Gao, R., Chen, X., & Kleywegt, A. J. (2017). *Wasserstein distributional robustness and regularization in statistical learning. arXiv preprint arXiv:1712.06050*.

Gao, R., & Kleywegt, A. J. (2016). Distributionally robust stochastic optimization with wasserstein distance. *arXiv preprint arXiv:1604.02199*.

Glasserman, P., & Yang, L. (2015). Bounding wrong-way risk in measuring counterparty risk. *Office of Financial Research Working Paper*, *15-16,* 15-76.

Green, A. (2015). *XVA: Credit, Funding and Capital Valuation Adjustments*. John Wiley & Sons.

Lichters, R., Stamm, R., & Gallagher, D. (2015). *Modern derivatives pricing and credit exposure analysis: theory and practice of CSA and XVA pricing, exposure simulation and backtesting*. Springer.

Matlab (2019). Matlab, counterparty credit risk and cva. `https://www.mathworks.com/help/fininst/counterparty-credit-risk-and-cva.htm` Accessed: 2019-07-30.

Memartoluie, A. (2017). *Computational methods in finance related to distributions with known marginals.*

Office of the Comptroller of the Currency (2011). Interagency supervisory guidance on counterparty credit risk management. *Bulletin 2011-30a*.

Ramzi Ben-Abdallah, M. B., & Marzouk, O. (2019). Wrong-way risk of interest rate instruments. *Journal of Credit Risk*, 21-44.

Singh, D., & Zhang, S. (2020). *Robust arbitrage conditions for financial markets. arXiv preprint arXiv:2004.09432*.